Optimization of Design, Growth, and Isolation of the RNA-Binding Protein G3BP1 for Solution State NMR and Biochemical Studies

By

NICKOLAUS BATROUNY
THESIS

Submitted in partial satisfaction of the requirements for the degree of

MASTER OF SCIENCE

in

Chemistry

in the

OFFICE OF GRADUATE STUDIES

of the

UNIVERSITY OF CALIFORNIA

DAVIS

Approved:

Dylan T. Murray, Chair

Sheila S. David

Andrew J. Fisher

Committee in Charge

2022

Acknowledgements

First, and foremost, I want to thank my sugar mama and wife, Hannah, for all her support during my academic journey over the last nine years. Without her love and encouragement, I would not have made it through all the ups and downs in my life. We are both looking forward to our lives after my project is finished so we can go back to experiencing a relationship of balance and selflessness that was absent throughout this process.

This thesis is dedicated to my nephews, Elias and Hezekiah, and my niece, Remi. I wanted to pave the way for their academic potential and leave no doubt in their minds they have the power to rise from their circumstances that have otherwise endured struggle and uncertainty in their futures. This is also dedicated to my mom, Wendy, and sisters, Scottie, Alex, and Holli, who were not able to be present during this journey away from home but have played a monumental role in my life and are the inspiration behind my determination to succeed.

I want to thank my roommate, lab-mate, and friend Khaled Jami for helping me through this project with the myriad issues that were ever-present. He trained me in the lab and was always available to help. We spent many-a-night talking over the next steps after the successes and failures, and I could not have made it this far with my project without him.

Finally, I want to thank Professor Dylan Murray for giving me the chance to finish my degree. I was days away from leaving Davis with nothing to show for the two and a half years of work I put into the program. I learned the reasons behind every step, and undoubtedly, am a better biochemist with more confidence and ability that will carry over into my next journey.

Abstract

As an RNA-binding protein, G3BP1 forms ribonuclear protein complexes with free mRNAs and proteins that leads to their separation from solution into biomolecular condensates. As a condensate, these species are removed from the processes of the cell thereby regulating transcription and metabolism which makes G3BP1 a compelling protein to study. In this paper, the foundation for producing isolated, *in vitro* G3BP1 is investigated for future spectroscopic and biochemical studies. Specifically, the human protein's sequence was inserted into an *E. coli* plasmid designed for heterologous expression and immobilized metal affinity purification. Afterward, the affinity tag was cleaved, and the protein was isolated from other contaminants as verified by SDS-PAGE. Since the solution pH and concentrations of G3BP1 and sodium chloride conflicted with those of spectroscopic studies, additional tests were conducted to uncover the favorable conditions. Optimization of the expression, purification, and cleavage of the affinity tag of G3BP1 was successful in isolating and producing large enough quantities of the full-length and intact protein for further experiments but maintaining the viable protein in buffers amenable to solution state NMR proved challenging.

Table of Contents

List of Abbreviations

AEX – Anion exchange chromatography

G3BP1 – Human Ras GTPase-activating protein-binding protein 1

HEPES – 4-(2-hydroxyethyl)-1-piperazineethanesulphonic acid

His – Histidine

HSQC – Heteronuclear Single Quantum Coherence

IDP – Intrinsically disordered protein

IDR – Intrinsically disordered region

IMAC – Immobilized metal affinity chromatography

LB – Lysogeny broth

MES – 2-(N-morpholino) ethane sulfonic acid

NHis-G3BP1 – Polyhistidine -tagged G3BP1 at N-terminus

Ni^{2+}-NTA – Nickel (II)-nitrilotriacetic acid

NTF2L – Nuclear transport factor 2-like domain

PIPPS – Piperazine-N, N′-bis (3-propanesulfonic acid)

RBP – RNA binding protein

RNP – Ribonuclear protein complex

RRM – RNA recognition motif

SDS-PAGE – Sodium dodecyl-sulfate-polyacrylamide gel electrophoresis

SEC – Size exclusion chromatography

SG – Stress granule

TB – Terrific broth

TEMED – Tetramethylethylenediamine

TEV – Tobacco etch virus

1. Introduction

RNA binding proteins (RBPs) in membrane-less organelles have garnered increasing curiosity and research efforts according to their importance in processes affecting DNA damage repair, stress granule (SG) formation and link to pathology in ALS.[1] This project aims to provide structural information about the RBP protein G3BP1 and its interactions by establishing a standard method that allows for future experiments involving its role in biomolecular condensates. Specifically, the project will identify optimal conditions for expression of the human protein heterologously in *E. coli*, establish multiple purification and analytical techniques for the protein, and test protein stability in several *in vitro* conditions. In doing so, the protein will be ready for structural characterization by NMR to elucidate how its conformational flexibility relates to its function in the context of various cellular systems.

1.1 Intrinsically Disordered Proteins

Proteins containing intrinsically disordered regions (IDR) make up over one half of known species of RNA chaperones, and one third of protein chaperones, while 44% of human protein-coding genes contain segments of greater than 30 amino acids in length predicted to be disordered.[2–5] It was initially thought that intrinsically disordered proteins (IDP) served only as linkers between structured proteins, but recent research is finding that these species impart cellular activities using multiple conformations or without well-defined conformations that challenge traditional structure/function ideology (Figure 1). Moreover, changes to their primary sequence via residue mutations that impact the region's fluidity are implicit in disease. A more detailed understanding of the possible conformations they sample and the role of these conformations in biological processes can lead to observable biomarkers that can be utilized to inform further treatments in targeted therapeutics. The current understanding of the

characterization of these IDRs is lacking, which provides opportunity to address this gap in knowledge.

Proteins containing IDRs have been difficult to visualize with typical biochemical techniques such as X-ray crystallography or cryogenic electron microscopy (cryo-EM) that require samples with well-defined shapes to produce measurements with high resolution. In particular, the variable conformational states of IDRs that exhibit dynamic interactions with ordered protein domains of globular proteins make structural characterizations difficult to obtain. Many proteins with IDRs have had their ordered domains structurally characterized, but analysis of the disordered regions resorts to tools such as AlphaFold that predict the three-dimensional structure that a protein will adopt based solely on its amino acid sequence. These tools decrease in the confidence of assigning residue coordinates within the folded protein as the regions become less structurally defined where confidence in the residue locations is completely lost for disordered regions. With the use of solution state NMR experiments, these IDRs can have the amino acid residue locations of their backbones assigned with respect to other residues within the disordered conformations. Using this information, binding studies such as inter and intra-protein interactions and post-translational modifications such as phosphorylation can be described more accurately.

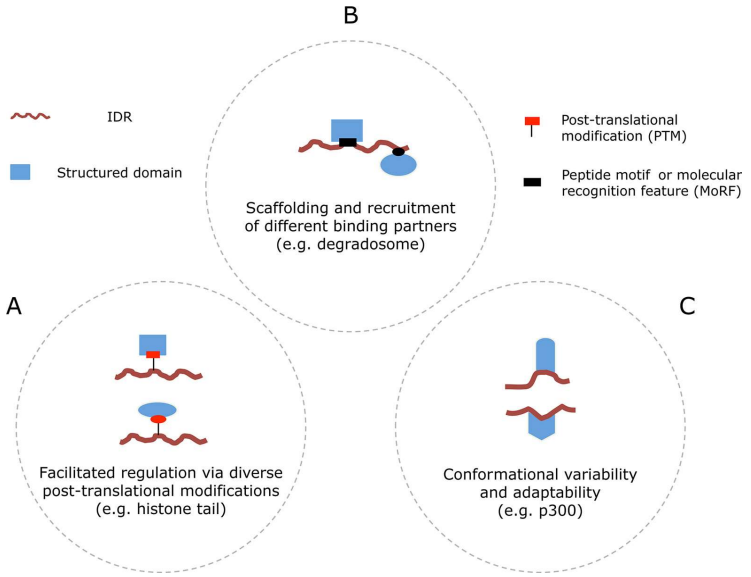

Figure 1. Classifications of IDRs according to their interactions. A) describes the ability of IDRs to bind to multiple partners during post-translational modification to facilitate distinct interactions between enzymes. B) shows the motifs within the IDRs that allow recruitment of different binding partners to increase their proximity. C) illustrates the conformational plasticity IDRs permitting their infidelity among globular protein binding sites. Figure reproduced from van der Lee et al. 2014

1.1.1 RNA-Binding Proteins

RNA-binding proteins (RBPs) are sometimes identified by well-structured RNA binding domains; however, IDRs have shown an affinity to bind to RNA without these conventional motifs. RBPs bind to RNA to form ribonuclear protein complexes (RNPs) that are primarily involved in gene expression. The dynamic composition of the RNP is directed by cellular needs dictated by the metabolic state of the cell such as controlling RNA decay and translation.[6] RBPs regulate many parts of RNA activity, including transcription, splicing, modification, intracellular movements, translation, and decay.[7] For example, the binding of RBPs to mRNA modulates available surface area which functions to regulate transcription.[8]

1.1.2 Biomolecular Condensates – Characterization and Attributes

Membrane-less organelles, or biomolecular condensates, are chemical enclosures in eukaryotic cells, like traditional organelles such as the endoplasmic reticulum, but lack external membranes. These organelles concentrate proteins and nucleic acids to drive diverse processes

such as RNA metabolism, DNA damage response and signal transduction. Complex biological reactions are accelerated or minimized in eukaryotic cells due to compartmentalization that can raise or spatially separate the local concentrations of metabolites and drive the direction of equilibrium. Organelles accomplish this feat with lipid bilayer membranes that sequester the components, and their presence is regulated through specialized membrane transport systems. Membrane-less RNP granules are biomolecular condensates that manifest when the RNPs are tasked with affecting the rate and direction of RNA metabolism within the cell. These granules exhibit a liquid-liquid phase separation (LLPS) which is brought about by localized condensation of proteins and nucleic acids. Granule formation is thought to be initiated by IDRs and has been observed in Cajal bodies, P bodies and stress granules (SGs).[9]

The research on P granules exposed the physical processes that underlie the formation of membrane-less enclosures of biomolecules. P granules were shown to be liquid-like droplets exhibiting LLPS properties that localize and condense proteins and nucleic acids into a dense phase through favorable entropic interactions.[10] Factors such as the concentration of biomolecular species and their identities along with environmental variables such as salt type (kosmotropic vs. chaotropic) and concentration, pH, and temperature can affect the condensation or dissolution of the liquid-like droplets.[11] The P bodies can fuse with one another, or dissolve into their original components, and allow proteins to mobilize within them or exchange with external species. Interactions between free metabolic partners such as RNAs and RBPs modulate the induction of LLPS due to increases or decreases in relative concentrations, multivalency, binding affinity, or solubility (Figure 2). At a critical concentration, the solubility limit of the metabolic partners is reached, and phase separation occurs. LLPS happens when multivalent components are brought together, and their translational entropy is reduced. However, the

conformational diversity of the macromolecule increases and is what drives assembly that, in turn, increases local concentrations beyond the solubility limit forcing the species to condense.[12]

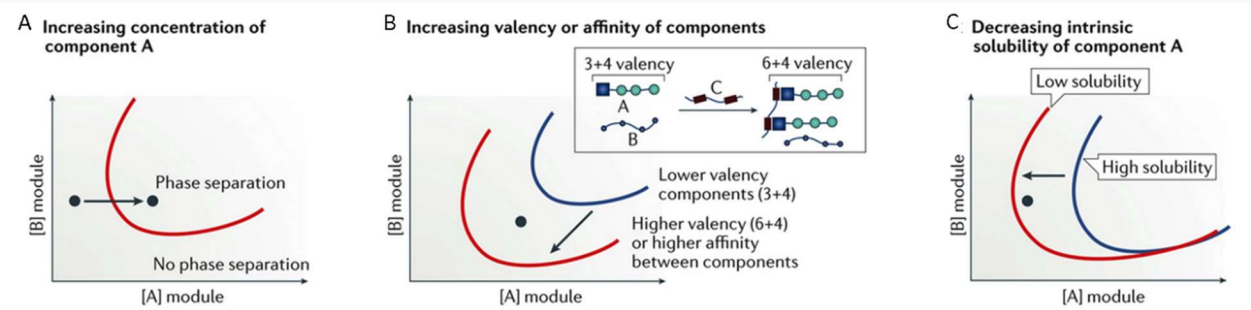

Figure 2: Phase diagram illustrating the modes of condensate formation between modules A and B arising from three functions: A) Increasing the concentration of A causes phase separation. B) Increasing the affinity or multivalency of A or B causes a phase separation (arrow) without changing the concentration. C) Decreasing the solubility of A enables condensation to occur with a fixed concentration. This figure was reproduced from Banani 2017

IDRs and low complexity domains promote phase separation due to their inherent multivalency and weak binding interactions. For example, repeating glutamine residues form collapsed structures in aqueous media due to the proximity of the polar moieties. These short-lived interactions are consistent with the dynamic behavior of LLPS and are involved in the formation of biomolecular condensates.

1.1.3 Stress Granules and Disease

Eukaryotic cells are exposed to a bevy of environmental stressors such as oxidative conditions, heat, hyperosmolarity, or UV irradiation and have a variety of methods to maintain homeostasis. Specific levels of metabolic precursors can lead to correct function within the cellular processes whereas an improper balance can overload the system meant to take care of the stress – leading to adverse effects. In response to stressors, the factors responsible for maintaining homeostasis can lead to recognizable and controllable effects such as post-translation or epigenetic modifications or the death of the cell, or apoptosis. Factors such as the upregulation of genes that move the equilibrium of metabolism forward can mitigate the effects of environmental stress, but only within the capabilities of the cell's regulatory capabilities. At

the point where the stress responses cannot keep up, damage manifests in a multitude of ways. When the stress or damage crosses the threshold of the capabilities of cell regulation, they lead to dysfunctional cell activity and apoptosis or senescence. Before the irreversible stages of apoptosis and senescence, there exist other forms of reversible regulation that can save the cell during periods of prolonged stress and inadequate shifts in equilibrium. These include systemic alterations such as changes to transcriptional activity through the physical formation of SGs.

SGs are membraneless organelles containing cellular metabolites that function to sequester important players in the cell cycle like proteins and free mRNA for the effect of slowing down the normal metabolic processes (like transcription) which can exacerbate the effect of cell stress if left unchecked. The main components of SGs are translation initiation factors, small ribosomal subunits, and a multitude of RNPs. When working appropriately, these SGs have been shown to form in cells introduced to heat shock by raising the temperature, and oxidative stress by adding sodium arsenite to cell culture media. The SGs are formed through reversible phase separation driven by RBPs that help sequester the ribosomal RNA, mRNA, and regulatory proteins to slow down protein synthesis in response to environmental stressors. For example, viral translation can be resisted by isolating the free mRNA into SGs during an infection, and post-translational modifications can be increased by the proximity of the requisite enzymes to their substrates.

1.1.4 Human Ras GTPase-Activating Protein-Binding Protein

Human Ras GTPase-activating protein-binding protein (G3BP) binds to the SH3 domain of the Ras-GTPase activating protein.[13] The G3BP family contains three homologous proteins G3BP1 and G3BP2(a/b), which are encoded by distinct genes.[14] Although the molecular conformation of G3BP proteins have not been modeled entirely, the amino acid sequence of

G3BP1 has produced insight on its characteristics as an RBP within the context of its multiple binding partners. The structure of the protein has unique qualities that are essential to the formation of RNP complexes such as an RNA recognition motif (RRM) for RNA binding and an arginine rich region that has shown to perform as stickers in enable physical crosslinking.[15] Past studies have linked G3BP1 to the formation and activity of SGs, where the phosphorylation of key residues within its central domain determines the fate of SG formation.[16,17]

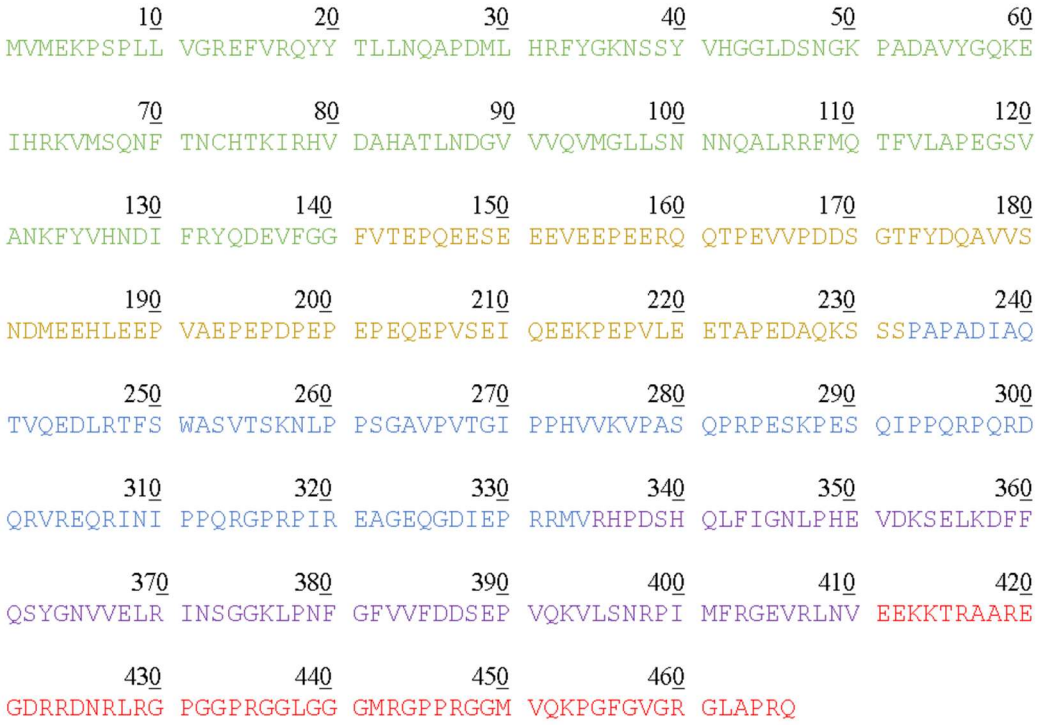

Figure 3: Highlighted G3BP1 full length amino acid sequence: nuclear transport factor 2 – like domain in green, intrinsically disordered region 1 in gold, intrinsically disordered region 2 in blue, RNA-recognition motif in purple and intrinsically disordered region 3 in red

G3BP1 is a 52 kDa protein containing five domains that consist of a nuclear transport factor 2-like (NTF2L) domain at the N-terminus followed by two IDRs (one acidic residue-rich and the other basic residue-rich), an RRM, and an RG-rich IDR at the C tail (Figure 3). The NTF2L domain is associated with nuclear transport and cellular localization and contains a

region that encourages dimerization. A rise in free RNA concentration and the interplay between the three IDRs influences the LLPS propensity of SG proteins, which is even more fine-tuned by phosphorylation within the core structure of G3BP1.[16] In addition to its IDRs, there exists regions of low complexity such as the RG-rich domain of IDR3 where the presence of multiply charged residues close together stimulate phase separation. Like in other RBPs, the RRM gives G3BP1 the ability to bind to mRNA to create RNP complexes that regulate processes in the cytoplasm using its multi-functional IDRs.

The NTF2L domain (residues 1-139) of G3BP1 has been crystalized and its structure modeled to an atomic resolution of 1.70 angstroms.[18] The remaining regions of the protein have only been predicted using Alphafold which is an AI system that predicts a protein's 3D structure from its amino acid sequence that regularly achieves accuracy competitive with experiment for proteins with well-defined structures.[19,20] Protein regions that have order, such as the NTF2L domain, achieve confidence scores above 90% whereas disordered regions correspond to per-residue confidence scores of less than 70% (Figure 4). These low-confidence regions predict primarily random coil structures that are mostly unfolded regions, solvent exposed, and contain no identifiable structure which opens the door to experimental structural studies such as solution state NMR to identify the proximities of the residues (i.e., local structural order) within the IDRs. When the molecular conformations sampled by G3BP1 in specific environmental contexts are known, binding studies can be implemented by tracking the changes to the structure after the introduction of relevant biomolecules. These changes can be interpreted to highlight the relevant amino acid residues with a variety of physiologically relevant binding partners to understand disease processes.

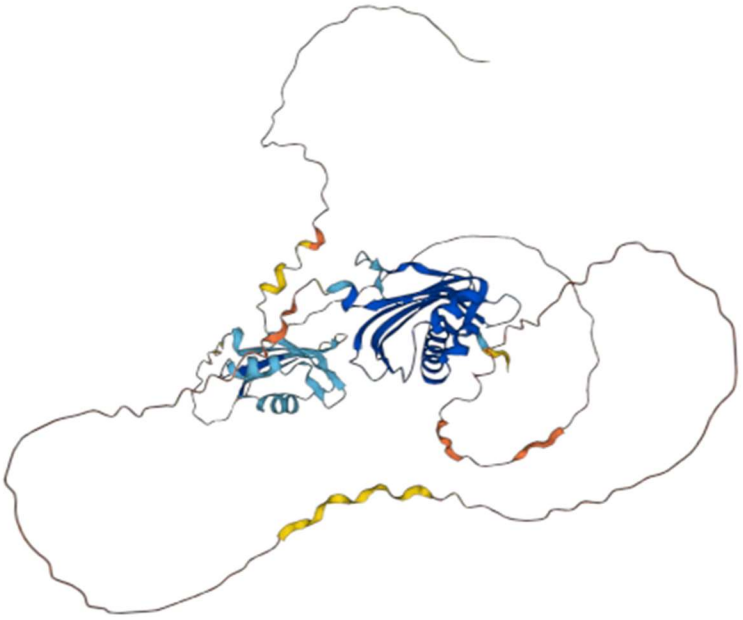

Figure 4: Predicted structure of Human G3BP1 (Q13283) from Alphafold with model confidence indicated by color: Dark blue = >90 %, Light blue = 70 – 90%, Yellow = 50 – 70 %, Orange = <50%

1.2 *In Vitro* Conditions of G3BP1 System

The following sections describe the methods used to obtain pure G3BP1 from the recombinant *E. coli* expression system. The human G3BP1 protein was recombinantly expressed in *E. coli* cells and purified *in vitro* based on the protocol established by Yang et al.[21] Outside of the cell, the protein is inherently less stable, and it is necessary to test conditions that will satisfy the solubility of the protein in solution during the techniques that are required to isolate it for structural studies. Specifically, the growth, expression, multiple purifications, and his-tag cleavage reaction with TEV need optimization for future work to establish a standard protocol. Additionally, obtaining high resolution solution state NMR data requires conditions that conflict with those of biological species including the buffer systems that will need to be tested for compatibility which is discussed in section 1.2.6.

1.2.1 pET11a-NHis-G3BP1 Plasmid and Expression System

The pET11a-G3BP1 plasmid was designed in-house using Genscript's GenSmart plasmid design tool with a pET11a vector backbone that was codon-optimized for an *E. coli* expression system (Figure 5). This plasmid was chosen as it conveys ampicillin resistance and has a T7 promoter system allowing for preferential antibiotic selection and temporal expression control by induction with IPTG. The NdeI cloning site was selected for its proximity to the ribosomal binding site. In addition to the G3BP1 full length protein, an N-terminal 6x histidine affinity tag was implemented for Ni^{2+} IMAC purification, and a cleavage site corresponding to the TEV protease was placed before the fusion protein.

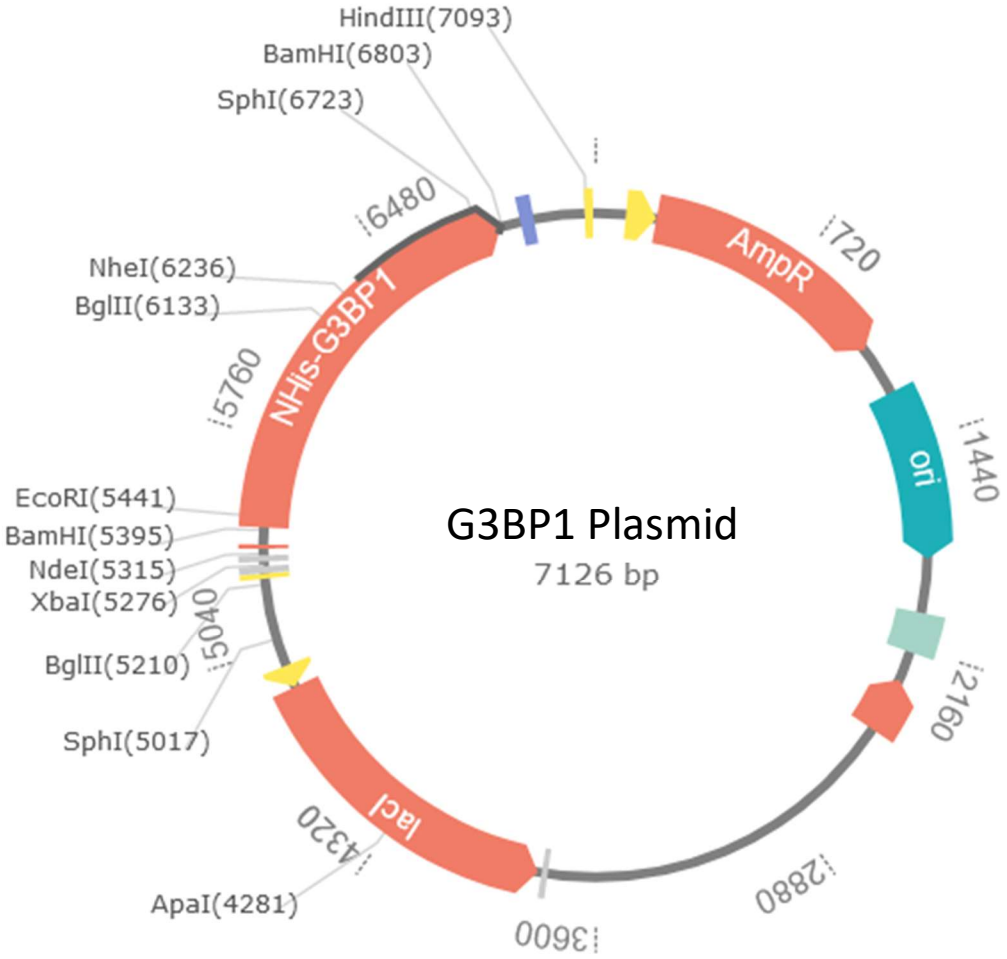

Figure 5: Circular map of pET11a-G3BP1 vector designed from GenSscript's GenSmart design tool including the ampicillin resistance promotor (AmpR), lac-operon repressor that is removed via IPTG induction (lacI), restriction enzyme at the N-terminal of the gene (NdeI) and the gene of interest (NHis-G3BP1).

1.2.2 Ni^{2+}-NTA Affinity Chromatography

Ni^{2+}-NTA affinity chromatography exploits the binding affinity of the imidazole side chain of histidine to the open site of the coordination sphere of Ni^{2+} bound to a nitrilotriacetic acid (NTA) chelating agent. Ni^{2+}-NTA resin columns are incubated with cell lysates and their components that contain recombinant proteins designed with his-tags to allow the chosen protein to bind selectively. After the undesirable species are introduced to the column, increasing concentrations of imidazole in the wash and elution buffers introduce competing interactions with the resin that displace the imidazole of the his-tag for protein collection. Since the pKa of histidine is close to 6, this technique is suitable for systems that are near physiological pH.

1.2.3 Anion Exchange Chromatography

Anion exchange chromatography (AEX) is possible when the pH of the protein buffer solution differs from the isoelectric point of the protein to be isolated. When the pH is above the isoelectric point, the protein has a net negative charge and has an affinity to positive species. When bound to a column of positively charged resin, the protein is immobilized while lesser-charged species interact with less affinity and can be removed during the wash step of purification. Removing the protein can be controlled by increasing the concentration of negatively charged species such as Cl^- ions that have a favorable interaction for the column and as the concentration of the Cl^- ions increases, the protein of interest is dislodged.

1.2.4 TEV Protease Affinity Tag Cleavage

Tobacco Etch Virus protease (TEV) is a 27 kDa 3C-type cysteine protease that can be used to remove affinity tags from recombinant proteins.[22] As a cysteine protease, TEV works by a catalytic triad composed of His46, Asp81, and Cys151 residues. Its substrate binding domain recognizes the amino acid sequence ENLYFQG and cleaves the peptide between glutamine and

glycine residues. The G3BP1 discussed in this paper was designed with a polyhistidine affinity tag to enable its isolation from the cell lysate after it is expressed in *E. coli* cells. Additionally, the pET11a-NHis-G3BP1 vector was designed with the ENLYFQG cleavage sequence preceding the full length G3BP1 protein sequence for the ability to study the native protein after TEV incubation and removal of the his-tag. TEV is combined with the isolated NHis-G3BP1 to cleave the affinity tag so that the studies of the full length, native G3BP1 do not include amino acid residues that will alter the protein's structure and characteristics in solution.

Enhancement of the native TEV protease has been obtained through specific point mutations that prevent self-proteolysis and increase the catalytic activity of the enzyme.[23] Optimal conditions of the TEV mechanism match physiological buffers such as pH and enable one TEV enzyme to cleave hundreds of substrates on the timescale of hours. Reverse Immobilized Metal Affinity Chromatography (Reverse IMAC) purification succeeding the cleavage process enables the G3BP1 protein to flow through the Ni^{2+}-NTA column rather than binding if the removal of the his-tag was successful. The TEV supply used in the lab contains an affinity his-tag of its own so that reverse IMAC purification of the protein accomplishes the result of isolating G3BP1 from its his-tag, uncleaved NHis-G3BP1 species, and the TEV protease. Using UV-vis to detect protein absorbance at 280 nm, the presence of protein in the flow through indicates successful cleavage of the affinity tag as the protein is unable to bind to the nickel column. SDS-PAGE gels also depict the cleavage success with an observable shift in location of the protein of interest by the mass difference of the his-tag (~3 kDa).

1.2.5 Size Exclusion Chromatography

Rather than chemical interactions, Size Exclusion Chromatography (SEC) relies on the physical properties of its resin to separate protein species according to their relative sizes in

solution, known as the hydrodynamic radius or Stokes radius. The protein solution is applied to a bed of resin with pores of varying size. Larger molecules enter fewer pores due to their larger hydrodynamic radius and therefore flow through the column faster. As a result, the larger components elute before the smaller ones and biomolecules are effectively separated based on their mass differences.

Each column has a unique elution volume or retention time for a given protein mass leaving the column. Protein standards with known masses are used to match protein size to elution times. Using an exponential curve fit to the standards' masses as a function of their elution times, it is possible to determine the size of the unknown sample eluates by comparison. However, these values can be distorted by protein structures that differ from globular proteins such as ones with intrinsically disordered regions as this increases their Stokes radius and alters their retention time within the resin matrix causing an increase in apparent molecular weight. When used correctly, and the molecular mass of the species is known, the elution time can provide evidence of monomeric or oligomeric structure or of other binding partners in solution due to the difference in mass between the protein of interest and its apparent weight. For example, if the weight is different by a multiple of the protein's weight, oligomeric structures can be deduced. This feature of SEC provides additional information in addition to increasing protein purity.

1.2.6 NMR Conditions for G3BP1 Samples

In addition to the signal-to-noise of NMR being proportional to the concentration of a particular species in solution, there exist conditions unique to biological samples that can impede the execution of accurate experiments such as sample concentration, salt concentration, and pH.

For this reason, tests were conducted on the purified G3BP1 protein for the optimal conditions to run NMR experiments.

After isolating G3BP1 from the cell lysate, it was necessary to test the purified G3BP1 in low salt conditions more amenable to NMR experiments. NMR relies on radiofrequency (RF) pulses to affect nuclear spins that precess at their larmor frequency and induce a measurable voltage that describes the chemical environment of the nuclei present in solution. The utility of NMR is enhanced by cryogenic probes that increase the sensitivity of these measurements by reducing the noise contribution of the receiver coils that detect the responses. Sample conductivity decreases this sensitivity enhancement and diminishes the signal-to-noise that is gained from near 0 K temperatures of the cryoprobe electronics.[24] In biological samples, this conductivity is present due to the buffers and salts that are necessary to stabilize the protein from aggregation and pH changes.

Just as importantly, the pH of a biological sample can affect the peak shape and, therefore, the sensitivity of the resultant spectrum. This is caused by chemical exchange between the protein of interest and its environment. Above its isoelectric point, the protein interacts with the chemical environment by rapidly exchanging protons that are undetectable by the NMR probe except as an average of the chemical shifts representing the bound and unbound proton states, leading to broad lineshapes and reduced peak intensities. At lower pHs this phenomenon is lessened which, in turn, results in sharper spectral peak shapes and larger peak intensities that are more useful in measuring the chemical shifts of the nuclei in the protein under study.[25] To increase the chance of obtaining high quality NMR spectra, sample concentration, salt concentration, and pH tests were conducted on the purified G3BP1 protein in solution for the optimal conditions to run NMR experiments.

1.2.7 ^{15}N NMR and Isotopic Labeling

Solution state NMR is a tool that is well-suited for the characterization of the molecular conformations sampled by IDRs with atomic resolution owing to their slower relaxation rates compared to larger, slower moving, globular biomolecules. Previous groups have produced a crystal of NTF2L and modeled the domain structure to an atomic resolution of 1.70 angstroms. However, as indicated by the Alphafold predicted structure in Figure 4, the remaining regions of the G3BP1 exhibit conformational plasticity, and their intrinsic disorder makes them less appropriate for techniques that require static shape. Solution state NMR is therefore an ideal technique to characterize the molecular motions and conformations sampled by the IDRs of G3BP1.

Traditional ^{1}H-detected NMR assignment strategies are complicated by IDRs with many domains containing tandem repeats of short oligopeptides with near-identical chemical shift patterns. Multidimensional experiments such as the 2D ^{1}H-^{15}N Heteronuclear Single Quantum Coherence (HSQC), take advantage of the greater chemical shift dispersion for ^{15}N nuclei compared with those of ^{1}H resonances and the 2D experiments provide increased resolution by spreading the signals out along another chemical shift dimension. Additionally, the HSQC experiment exploits the slower transverse relaxation property of ^{15}N nuclei that provide a narrower linewidth with a corresponding increase in signal height and sensitivity compared to that of ^{1}H and ^{13}C nuclei.[26] Except for proline, every amino acid residue within a protein contains a backbone primary amine and attached amide proton. In HSQC each amide yields a peak in the spectra by producing a correlation between the primary nitrogen and amide proton (Figure 6).[27] This makes it possible to assign backbone resonance peaks to the unstructured regions of the protein.

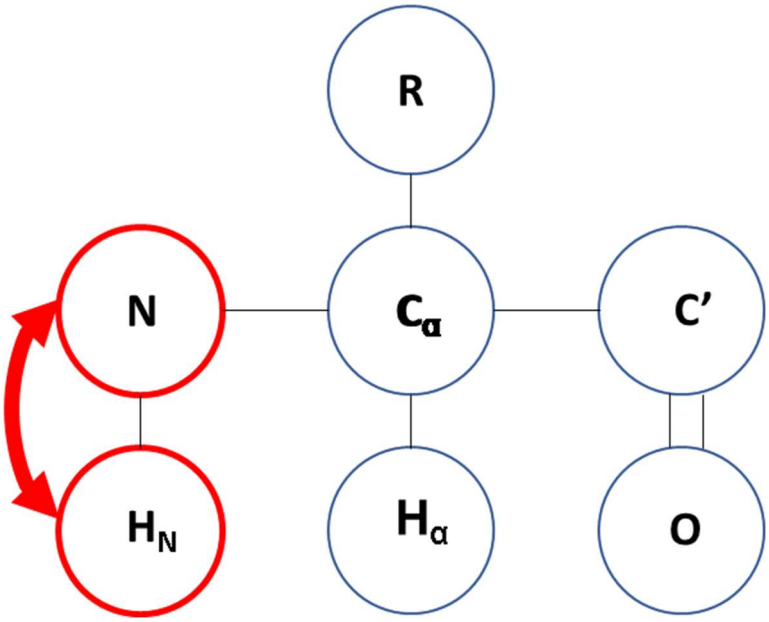

Figure 6: Schematic representation of 1H–15N HSQC polarization transfer between amide proton and nitrogen of a generic amino acid where the polarization begins at the proton of the amide (HN) and transfers to the nitrogen (N) before it is transferred back to the amide proton to record the signal.

The natural abundance of the isotope ^{15}N is 0.368%.[28] The sensitivity of the ^{1}H-^{15}N-HSQC technique is therefore reduced for the naturally occurring isotope distributions in proteins and requires an additional step of expressing the gene of interest in an isotopically enriched minimal media. This is accomplished by growing the *E. coli* cell cultures to high cell densities in rich (natural abundance) media, harvesting the cells, washing away the rich media, and introducing the cells into a minimal media containing $^{15}NH_3$ as the sole nitrogen source before induction and expression of the protein. Because the labeled ammonia is the only source of nitrogen within the media and induction is delayed until after its introduction, the synthesis of the protein in the cells uses amino acids enriched with ^{15}N nuclei. Replacing the nitrogen atoms within the protein of interest with ^{15}N atoms has the effect of increasing the sensitivity of ^{15}N-NMR experiments such as ^{1}H-^{15}N-HSQC.

1.3 Research Goals

The G3BP1 protein is found in SGs that can convert into harmful condensates when the metabolic precursors within the cell reach stressful levels and the SG rigidifies, lead to pathological fibril formation.[1] So far, the structure of the full-length protein has eluded spectroscopic techniques aimed at defining the proximities of the intrinsic residues that lead to a better understanding of the protein's secondary and tertiary interactions underlying SG formation. When the locations of the interacting residues are known within the structure, binding studies can be performed with cellular metabolites such as nucleic acids and proteins and the changes to the structure can define biomarkers of harmful interactions that can be diagnosed in clinical settings. It is the goal of this research project to establish a protocol to produce and isolate the G3BP1 protein in amounts large enough for these biochemical and spectroscopic studies. Beginning with the plasmid vector design, an entire step-by-step method needs developing whereby the plasmid is grown and expressed in *E. coli* cells, extracted, and isolated from the cell lysate and maintained *in vitro* with conditions suitable for extended storage and subsequent experimental analysis. In addition to isotopic labeling and growth of ^{15}N-enriched G3BP1, NMR-relevant condition tests are necessary to conduct since the known buffer compositions that keep G3BP1 soluble contrast with those required for NMR experiments. As an added benefit of purification protocols using SEC, the quaternary structural state of the G3BP1 protein in solution will be obtained. Taken together, the work provided in this paper is intended to build the foundation for future structural studies that will elucidate a better understanding of the protein system that address its context in diseases such as ALS.

2 Materials

Solutions were prepared with nanopure water and sterile filtered through 0.22 μm bottle top filter units or autoclaved at 121 ℃ for 30 minutes before use.

List of Reagents

Item (Alphabetical)	Brand	Item #
Glycerol	Fisher	BP229-1
Glycine	Fisher	BP381-1
Sodium Chloride	Fisher	BP358-1
Pierce™ Protease Inhibitor Mini Tablets, EDTA-free	Thermo	A32955
Potassium phosphate monobasic	Fisher	BP362-1
SDS Pellets	Fisher	BP8200-500
Sodium phosphate dibasic heptahydrate	Fisher	S373-500
Sodium phosphate monobasic anhydrous	Fisher	BP329-1
TEMED	Fisher	BP150-20
Tricine	Sigma Aldrich	T0377-1KG
Tryptone	Fisher	BP1421-500
Yeast Extract	Acros	451120010
Glucose	Thermo	A168280E
GeneJET Plasmid Miniprep Kit	Thermo	K0502
Acrylamide: Bis-Acrylamide 37.5:1	Fisher	BP14101
Ethanol	Fisher bioreagents	BP8202-4
Imidazole	Fisher	BP305-50
Tricine	Fisher	BP315-100
Hydrochloric Acid Concentrate	Fisher	AC423795001

Ribonuclease A, bovine pancreas, purified	Alfa Aesar	J61996-MB
Deoxyribonuclease I, bovine pancreas	Alfa Aesar	J62229-MB

Consumables

Item	**Brand**	**Item #**
Dialysis tubing (3.5 kDa mwco/6.4mL/cm)	Fisher	132724
SEC column protein standards	Bio Rad	1511901
SDS-PAGE Protein Ladder	Pageruler unstained protein ladder	26619
0.22 μm Filter	ELGA	LC145

Solutions for Protein Work

Solution	**Protocol/Contents**
NHis-G3BP1 IMAC equilibration buffer	50 mM HEPES, 250 mM sodium chloride,1 mM DTT, pH 7.5
Lysis buffer	0.25 μg/mL R-Lysozyme, 0.1 μg/mL RNase, 0.01 μg/mL DNase, and 1% (v/v) Triton X-100 final concentrations and 1 protease inhibitor tablet/10 mL were added to equilibration buffer
NHis-G3BP1 IMAC wash buffer	25 mM Imidazole final concentration was added to NHis-G3BP1 IMAC equilibration buffer
NHis-G3BP1 IMAC elution	500 mM Imidazole final concentration was added to NHis-

buffer	G3BP1 IMAC equilibration buffer
TEV lysis buffer	20 mM Tris-HCl, 500 mM sodium chloride, .25 mg/mL R-Lysozyme at pH 8.0 final concentrations
TEV equilibration buffer	20 mM Tris-HCl, 500 mM sodium chloride, and 20 mM Imidazole at pH 8.0 final concentrations
TEV wash buffer	TEV Equilibration Buffer with 80 mM Imidazole
TEV elution buffer	TEV Equilibration Buffer with 500 mM Imidazole
SEC running buffer	50 mM HEPES, 250 mM sodium chloride,1 mM DTT, pH 7.5
LB media	10 g tryptone, 5 g yeast extract and 10 g sodium chloride were added to 1 L water and autoclaved
TB media	20 g tryptone, 24 g yeast extract, 4 mL glycerol, 9.8 g Na_2HPO_4 and 3 g KH_2PO_4 were added to 1 L water and autoclaved
LB agar plates	50 mL LB Media was supplemented with 1 g Agar
M9 media	12.27 g $Na_2HPO_4 \cdot 7H_2O$, 2.7 g KH_2PO_4 and 0.5 g sodium chloride were added to a final volume of 1 L water at pH 7.2 and autoclaved. 1.0 g $^{15}NH_4Cl$, 2 mL 1M $MgCl_2$, 100 µg/mL ampicillin, and 100 µL 1M $CaCl_2$ were then mixed with 50 mL 20% (w/v) glucose and added before use
4x SDS	10 mL 0.5 M Tris pH 6.8, 8 mL glycerol, 1.6 g SDS pellets and 0.04 g Bromophenol Blue were mixed with 1 mL water
4 % polyacrylamide gel	600 µL 40% Bis-acrylamide (v/v), 1.5 mL 0.5 M Tris-HCl pH 6.8, 60 µL 10% SDS (v/v), 30 µL 10% (v/v) APS and 12 µL TEMED were added to 3.8 mL water
10 % polyacrylamide gel	2.5 mL 40% Bis-acrylamide (v/v), 2.5 mL 1.5 M Tris-HCl pH 8.8, 100 µL 10% SDS (v/v), 50 µL 10% (v/v) APS and 10 µL TEMED were mixed with 4.8 mL water

4-10 % gradient polyacrylamide gel	2.5 mL 4% polyacrylamide gel solution was drawn into a serological pipette followed by 4 mL of 10% polyacrylamide gel solution and mixed by aspirating air with pipette controller
Fixing solution	100 mL glacial acetic acid and 500 mL methanol mixed with 400 mL water
Coomassie stain	Dissolve 2.5 g of Coomassie Brilliant Blue G-250 in 500 mL of methanol and stir for 3 hr. Add 400 mL of water and 100 mL of glacial acetic acid. Stir for 15 minutes
Destain solution	70 mL glacial acetic acid and 120 mL methanol mixed with 810 mL water
Staining solution	50% Coomassie in Fixing solution (v/v)
10x Tricine running buffer	1 M Tris-HCl, 1 M tricine and 1% (w/v) SDS in water
0.2 M Tris-HCl tank buffer	0.2 M Tris-HCl pH 8.8 in water

Purification and Analysis Equipment

Instrument/Attachment	**Supplier**	**Product Number**
FPLC – NGC Medium Pressure Liquid Chromatography System	Bio Rad	7880009
Anion column – UNO Q6 Column	Bio Rad	7200003
Nickel IMAC column – EconoFit Profinity IMAC Columns, 5 mL Ni-charged	Bio Rad	12009300
Ni^{2+}-NTA resin – Nuvia IMAC resin	Bio Rad	7800802
SEC column – ENrich SEC 650 10 x 300 Column	Bio Rad	7801650

PAGE cell – Mini-PROTEAN Tetra Vertical	Bio Rad	1658004
GeneJET Plasmid Miniprep Kit	Thermo Scientific	K0502

Cell Lines and Vectors

Name	**Host**	**Description**	**Supplier**
BL21(DE3) cells	*E. coli*	Ca^{2+} competent expression system	Prepared in-house
DH5alpha cells	*E. coli*	Ca^{2+} competent plasmid amplification system	Prepared in-house
pET11a-G3BP1	*E. coli*	G3BP1 expression vector	GenScript
MBP-HIS-TEV plasmid	*E. coli*	Protease system for affinity tag removal	Courtesy of Prof. T. A. Cross, Florida State University

3 Methods

3.1.1 pET11a-NHis-G3BP1 Plasmid Synthesis

G3BP1 – expressing constructs (Human Ras GTPase-activating protein-binding protein – primary accession Q13283) contained a TEV cleavage site between the N-terminal, 6xHis-tag, and fusion protein (MSYYHHHHHHDYDIPTTENLYFQGAMDP). The plasmid was constructed from a pET11a vector containing a T7 promoter system and ampicillin resistance marker and the gene with N-terminal 6xHis-tag was inserted at the NdeI cloning site. The nucleic

acid sequence was codon optimized for an *E. coli* expression system and ordered from Genscript.

3.1.2 Amplification and Transformation of pET-DH5α-NHis-G3BP1

The DNA plasmid was delivered as a 4 μg lyophilized powder and resuspended according to the manufacturer's directions. The pET11a-NHis-g3bp1 plasmid was transformed into Ca^{2+}-competent DH5α *E. coli* cells by adding 2 μL of the resuspension and incubating the cells for 15 minutes on ice. The mixture was subsequently incubated at 42 °C for 90 seconds and then incubated for another 2 minutes on ice. 500 μL of LB media was then added to the mixture and placed in a shaker incubator for 30 minutes at 37 °C and 220 rpm for plasmid amplification. 25 μL and 125 μL aliquots were streaked over two agar plates containing 100 μg/mL ampicillin and allowed to incubate at 37 °C overnight. After growth, two colonies (#1 and #2) from either plate were selected used to inoculate two separate 12 mL preparations of LB media with 100 μg/mL ampicillin and grown overnight in a shaker incubator at 37 °C and 220 rpm. Equal parts culture and 50 % sterile filtered glycerol were mixed to prepare glycerol stocks of each culture the following day, flash-frozen in liquid nitrogen, and storing at −80 °C.

Purified DNA was extracted from the DH5α *E. coli* cells using the Thermo Scientific GeneJET Plasmid Miniprep Kit and following the manufacturer's directions. The resultant bacterial culture was centrifuged for 10 minutes at 6000 x*g* and the pellet was resuspended in Resuspension Solution. The resuspension was lysed and neutralized before adding to the Thermo Scientific GeneJET Spin Column. The column was washed twice before being placed into a new microcentrifuge tube where the elution solution was added and the flow through was collected. The concentration of the elute was calculated by measuring the A_{260} and using an average ε_{260} of

50 ng/µl per 1.0 absorbance units. The samples were then diluted to 80 ng/µl and stored at −20 °C.

3.1.3 Growth of pET-BL21(DE3)-NHis-G3BP1

Expression of the NHis-G3BP1 protein used the amplified pET-NHis-G3BP1 plasmid and BL21(DE3) Ca^{2+}-competent *E. coli* cells. Transformation and additional plasmid amplification were performed identically to that of the Ca^{2+}-competent DH5α *E. coli* cells and 25% glycerol stocks (final concentration) were prepared and frozen at −80 °C. The glycerol stock was used for successive growths as described previously. Growth was initiated by using a pipette tip to streak a small amount of the BL21(DE3) glycerol stock over LB agar plates containing 100 µg/mL ampicillin and incubating overnight at 37 °C. Single colonies were used to inoculate 500 mL LB culture containing 100 µg/mL ampicillin and incubated overnight at 37 °C without shaking. A volume of the small cultures was then added to 1 L LB cultures containing 100 µg/mL ampicillin to achieve a A_{600} of 0.1. The culture was then grown in a shaker incubator at 37 °C and 220 rpm.

3.1.4 Expression of pET-BL21(DE3)-NHis-G3BP1

Expression of the protein was induced in the large cultures at an A_{600} of 0.6–0.8 by adding IPTG to 0.5 mM. The cultures were grown for an additional 4 hours at 37 °C and 220 rpm. Every hour samples were removed from the 1 L large cultures to prepare SDS-PAGE samples for monitoring the protein expression and the aliquot volumes were calculated by 500 µL/A_{600}. The culture was pelleted at 14000 x*g* for 10 minutes, the supernatant discarded, and the pellet resuspended in a 100 µL of 1 x SDS sample buffer. The large-scale cultures were harvested after 4 hr growth at 37 °C by centrifuging at 6000 x*g* for 10 minutes at 25 °C. The pellets were weighed (~ 2 – 4 g each), flash-frozen in liquid nitrogen, and stored at −80 °C.

3.1.5 Growth and Expression of ^{15}N-labeled pET-BL21(DE3)-NHis-G3BP1

Growth of ^{15}N-labeled pET-BL21(DE3)-NHis-G3BP1 was performed the same as non-labeled culture, but the LB media was supplemented with 1 % (w/v) glucose in the small and large cultures to prevent expression of the protein prior to induction with IPTG. After reaching an A_{600} of 0.8, two 1L cultures were pelleted at 6000 x*g* for 10 minutes at 25 °C. The pellets were resuspended in 1 L M9 media before being placed in a shaker incubator and grown at 37 °C and 220 rpm for 30 minutes. Afterwards, 0.5 mM IPTG was used to induce expression of the protein. The expression was monitored with SDS-PAGE samples normalized to their respective A_{600} as described in section 3.1.4. After 3 hours of expression, the cultures were pelleted at 6000 x*g* for 10 minutes at 25 °C. The pellets were weighed, frozen in liquid nitrogen, and stored at -80 °C.

3.1.6 Lysis and IMAC Purification of NHis-G3BP1 from pET-BL21(DE3)-NHis-G3BP1

Frozen cell pellets were resuspended in 10 mL lysis buffer per gram of pellet and sonicated in 50 mL plastic tubes on ice. Sonication was performed twice with settings: Pulse Mode, 0.30 seconds on, 3.0 seconds off, 1.0 min Total On, at 30 % power. The sonicated cell lysates were pelleted at 30000 x*g* at 4 °C for 30 minutes. The supernatants were syringe-filtered through a 0.22 μm filter unit and loaded onto a 5 mL Ni^{2+}NTA IMAC column equilibrated with equilibration buffer and run on a bio rad NGC FPLC. The column was then washed and eluted in equilibration buffer with an imidazole gradient starting at 20 mM and ending at 500 mM. Lysate, supernatant, flow through, wash, and elution samples were analyzed by SDS-PAGE before pooling the elution fractions containing pure NHis-G3BP1 protein. These fractions were dialyzed at 4 °C against equilibration buffer to remove the imidazole. After each purification, the IMAC column was stripped and recharged according to the manufacturer's protocol.

3.1.7 His-Tag Cleavage by TEV Protease

A_{280} measurements were taken of the dialyzed samples and used to assess the concentrations according to the extinction coefficient of NHis-G3BP1 at 280 nm (24870 $M^{-1}cm^{-1}$). NHis-TEV was added to the dialysis tubing at a 1:50 (TEV:G3BP1) molar ratio and placed in fresh dialysis at 4 °C for 48 hours. Samples were taken throughout the cleavage process and analyzed with SDS-PAGE (section 3.3) for his-tag-cleavage efficiency.

3.1.8 Reverse IMAC Purification of G3BP1

Nickel IMAC resin was added to a gravity column and equilibrated with dialysis (equilibration) buffer. The mixture of G3BP1 and TEV were added to the column and stored at 4 °C for 1 hour before collecting the flow through. The column was washed with wash buffer (section 2) equal to the volume of the flow through and collected. The column was then washed with elution buffer (section 2) until the A_{280} reached baseline. The flow through, wash and elution elute fractions were analyzed with SDS-PAGE (section 3.3) for identification of the purified product, and the his-tag-cleaved G3BP1 fractions were pooled, dialyzed against equilibration buffer FOR HOW LONG, and stored at 4 °C for short term use. Quantification of the cleaved G3BP1 yield was determined with an A_{280} extinction coefficient of 18910 $M^{-1}cm^{-1}$ that was calculated using the PROTPARAM tool on the ExPASy server.[29]

3.1.9 Size Exclusion Analysis of G3BP1

SEC analyses were performed on the FPLC equipped with SEC 70 and 650 columns equilibrated with SEC running buffer and ran at 1.0 mL/min. Purified proteins were concentrated using microcentrifuge spin filters to 60 µM in running buffer before 0.22 µm syringe filtering to remove any insoluble particulate and loaded onto a 250 µL injection loop on the FPLC. The sample was injected on the column by running 1 mL of running buffer through the injection loop

to ensure all protein made its way onto the column. For size analysis, elution times of the protein were compared to SEC column protein standards that were previously run according to the exponential curve fit using Excel (Mass = 501486.3*$e^{(-.65x)}$ +-2.1) where 'x' is the retention time.

3.2.1 Growth and Expression of TEV-T Protease

Frozen glycerol stock of TEV-T BL21(DE3) cells was streaked over LB agar plates containing100 µg/mL ampicillin using a pipette tip and incubated overnight at 37 °C. Single colonies were used to inoculate a 500 mL TB media culture containing 100 µg/mL ampicillin and incubated quiescently overnight at 37 °C. 100 mL of the overnight cultures were then added to 900 mL of the TB media containing 100 µg/mL ampicillin before growing in a shaker incubator at 37 °C and 220 rpm to an A_{600} of 0.6–0.8. The temperature was then reduced to 20 °C and expression of the TEV induced with 0.5 mM IPTG for 18–20 hours. The final A_{600} was 9.0. The cells were spun at 6000 x*g* for 10 minutes and the pellets were weighed, flash-frozen in liquid nitrogen, and stored at −80 °C. Samples were taken during the growth at just before harvesting the cells, normalized according to the respective A_{600}, and analyzed with SDS-PAGE.

3.2.2 Lysis and Purification of TEV-T BL21(DE3) Protease

Frozen cell pellets were resuspended and sonicated in TEV lysis buffer on ice in a plastic 50 mL conical tube. Sonication was performed twice with settings: Pulse Mode, 0.30 seconds on, 3.0 seconds off, 1.0 min Total On, at 30 % power. The sonicated cell pellets were centrifuged at 75600 x*g* at 4 °C for 30 minutes. The supernatants were syringe-filtered through a 0.22 µm filter unit and loaded onto a Nickel IMAC FPLC column equilibrated with TEV equilibration buffer. The column was then washed and eluted with respective TEV buffers (section 2). After purification, the IMAC column was stripped and recharged according to the manufacturer's protocol. Lysate, supernatant, flow through, wash and elution samples were analyzed by making

SDS-PAGE samples and imaging (section 3.3) before pooling the elution fractions containing the pure TEV protein. The purified TEV protein solutions were stored at −80 °C in 250 mM sodium chloride, 10 mM Tris-HCl, 250 mM Imidazole, 1 mM EDTA, 5 mM DTT and 50 % glycerol (v/v) final concentrations by diluting the sample two-fold with 100 % glycerol. A_{280} measurements were taken of the dialyzed samples and used to assess the concentrations according to the extinction coefficient of TEV at 280 nm (33710 $M^{-1}cm^{-1}$).

3.3 SDS-PAGE

SDS-PAGE was used to separate proteins according to molecular weight for component identification. The electrophoresis apparatus was assembled according to the manufacturer's instructions with the upper reservoir containing 1x tricine running buffer and the lower reservoir holding 0.2 M Tris-HCl tank buffer. SDS-PAGE gels were made from 4–10 % polyacrylamide gel solution poured between two glass plates and allowed to dry with 15-lane ladder inserts before storing at 4 °C. Protein samples were added to 3-fold-diluted 4x SDS (e.g., 10 µL protein solution with 20 µL water and 10 µL 4x SDS). Growth and expression samples were normalized to A_{600} = 500 A.U.* (µL of culture), pelleted at 6000 x*g* for 10 minutes and reconstituted in 1X SDS solution. The samples were heated at 90 °C for 10 minutes before centrifuging at 14000 x*g* for 2 minutes to separate any insoluble material. The ladder was added as 5 µL into the lanes along with the Sample lanes were loaded with volumes between 5–10 µL and 5 µL of the protein ladder added to an additional lane for calibration of the gel. The gel was run at 45 mA until the bromophenol blue front reached the bottom of the gel. Afterward, the gels were rinsed with water, stained in staining solution for 15 minutes, and destained in destaining solution for up to an hour before imaging.

4 Results and Discussion

4.1 pET11a-NHis-G3BP1 Plasmid

The pET11a-NHis-G3BP1 vector was obtained from GenScript as a lyophilized powder that required transformation into two strains of *E. coli* cells (DH5α and BL21(DE3)) capable of plasmid amplification and gene expression, respectively, with the intent of producing enough protein for biochemical and spectroscopic studies.

4.1.1 pET11a-NHis-G3BP1 Plasmid Transformation

First, the vector was resuspended in water and transformed into Ca^{2+}-competent DH5α *E. coli* cells which can be heat-shocked for plasmid intake and are specialized for high efficiency plasmid transformation and amplification. After the cells were grown, the amplified plasmid was extracted using the GeneJET Plasmid Miniprep Kit and the amount of DNA was calculated using the absorbance at 260 nm where 1.0 A.U. = 50 ng/mL (plasmid from culture #1 = 83 ng/μL and plasmid from culture #2 = 89.8 ng/mL). These two samples were Sanger sequenced, and the results indicated a match with the desired G3BP1 protein sequence.

The extracted plasmids were then transformed into Ca^{2+}-competent BL21(DE3) *E. coli* cells which are suitable for high-level T7 expression of recombinant proteins. After transformation, the cells were grown to increase the cell density, and glycerol stocks were made of the two cultures and stored in 25% glycerol (v/v) as a cryoprotectant at −80°C for subsequent growths and expressions. The BL21(DE3) strain carries the gene for T7 RNA polymerase under control of a lacUV5 promoter. This polymerase controls the regulation of gene expression within the cell and is turned on with IPTG which is responsible for the expression of the NHis-G3BP1 protein. Additionally, the strain is engineered without the regulatory, ATP-dependent lon protease and outer membrane protease OmpT. These two proteases are responsible for

degradation of heterologous proteins expressed in the cells and their removal protects full-length NHis-G3BP1 after it is produced.[27,28]

4.1.2 Optimization of pET11a-BL21(DE3)-NHis-G3BP1 Expression

Growth and expression of the pET11a-G3BP1 vector was optimized via small scale expression tests that were conducted to determine the most effective length of expression and culture temperature for obtaining the highest yield of the protein. Temperature and time combinations of 37 ℃ for 2, 4 and 6 hours, and 20 ℃ for 20 hours were assessed and their respective SDS-PAGE samples were compared against cultures lacking IPTG (Figure 7). There was no observable difference between the two highest yielding temperature and time combinations regarding the darkness of their bands. The cultures grown at 37 ℃ for 4 and 6 hours were the most effective at growing protein so the shorter of the two times was selected for future expressions.

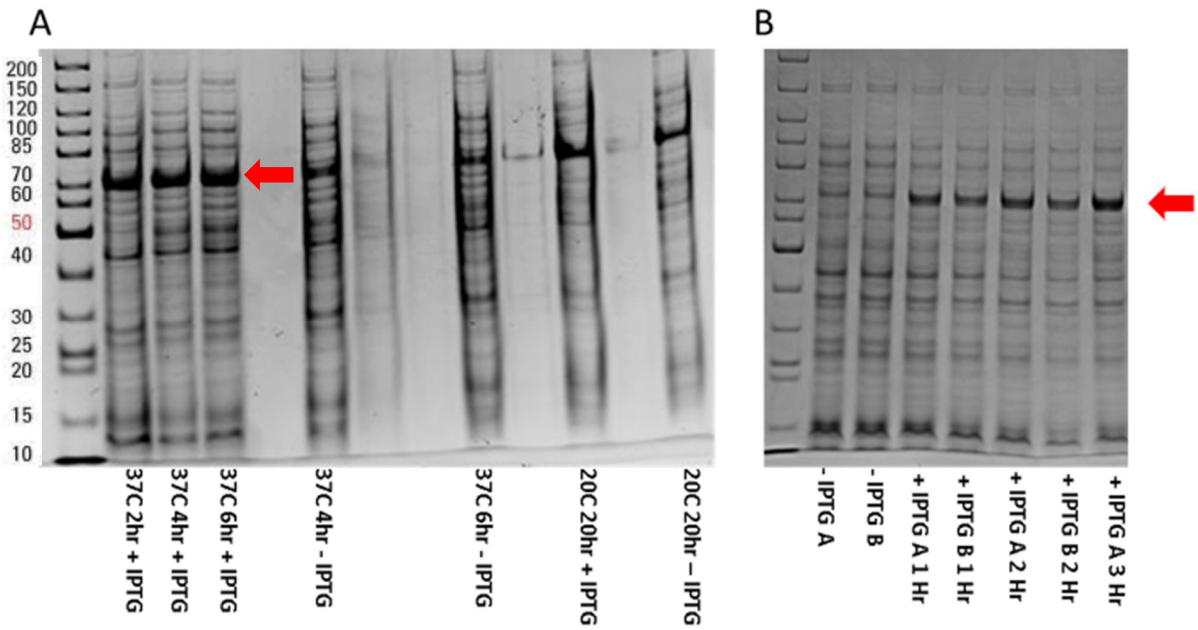

Figure 7: Expression of NHis-G3BP1 – A is the SDS-PAGE gel of the small-scale expression tests of NHis-G3BP1 where IPTG was added to the cultures at 37 °C for 2, 4, and 6 hours and 20 °C for 20 hours and compared to cultures without IPTG as controls. The red arrows are pointing at the band of NHis-G3BP1 near 70 kDa. B is the SDS-PAGE gel of the large-scale expression of NHis-G3BP1 at 37 °C for 3 hours with samples taken from cultures A and B.

4.1.3 Optimization of pET11a-BL21(DE3)-NHis-G3BP1 IMAC Purification

The purification of NHis-G3BP1 was developed after the protocol established by Yang et al. for *in vitro* purification of full length G3BP1.[18] It was necessary to isolate the protein from the *E. coli* cells where the protein was expressed in order to perform experiments on the structure of full length G3BP1. The first purification technique is immobilized metal affinity chromatography (IMAC), which is a process that separates proteins designed with a his-tag such as NHis-G3BP1 from other components of the cell lysate.

The G3BP1 protein was purified from the cell pellets of the 4- and 6-hour small scale expression by loading the supernatant of the lysed cell pellets with Ni^{2+} NTA resin in microcentrifuge tubes and incubating on ice for 15 minutes. After centrifuging for 2 minutes at 14000 x*g*, the supernatant was collected. This was followed by adding five separate column volumes of wash buffer, centrifuging for 2 minutes at 14000 x*g* after each addition and collecting

the supernatants from the column. An additional five separate column volumes of elution buffer were added and centrifuged for 2 minutes each at 14000 x*g* and collected. The wash and elution collections from the column were then analyzed with SDS-PAGE to determine the relative presence and purity of G3BP1. Figures 8A and 8B show the band corresponding to NHis-G3BP1 is most prevalent in the elution fractions near 70 kDa.

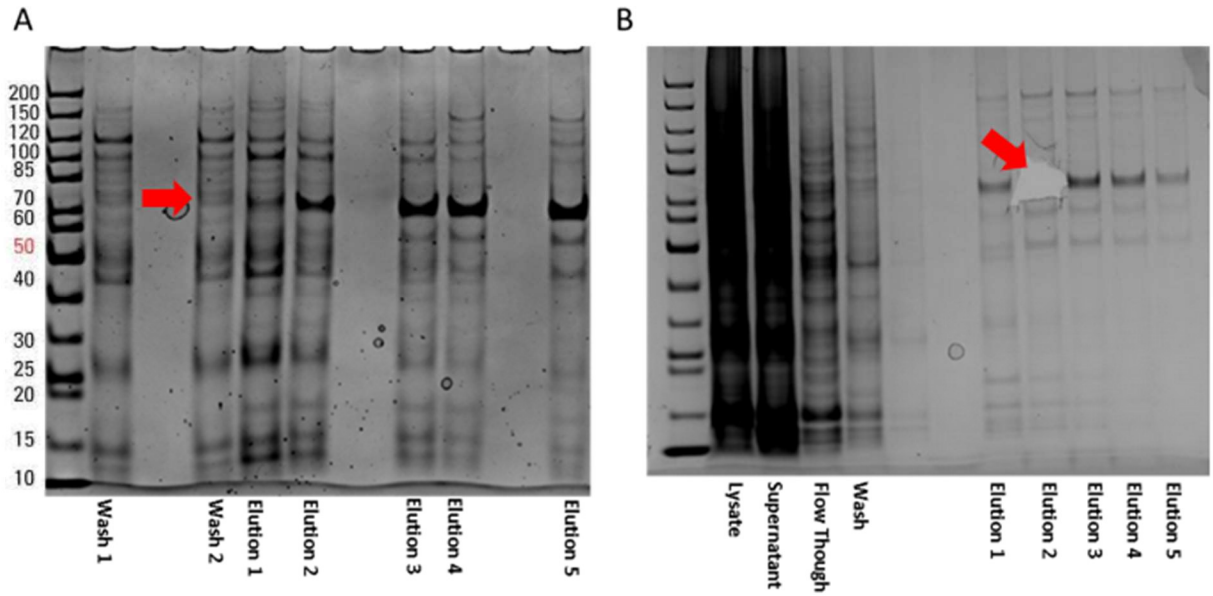

Figure 8: SDS-PAGE gels of two IMAC purifications from cell lysates – A shows the results from the purification of the 6 – hour small scale expression sample where the red arrow indicates the location of bands corresponding to NHis-G3BP1 throughout the wash and elution steps. B shows the results from the purification of the 4 – hour small scale expression sample where the red arrown indicates the incision location from the gel that was extracted for sequence identification.

Equipping the protein with a his-tag enabled it to bind to the IMAC resin column and be removed with high imidazole concentrations in the elution steps. The ability of the tag to bind to the column was evident in the amount of protein found in the elution fractions compared to the wash in Figure 8. There was a significant size disparity between the predicted molecular weight of NHis-G3BP1 (55 kDa) and the most prevalent band on the gels (70 kDa). Consequently, the 70 kDa band from the elution 2 sample was extracted from the gel in Figure 8B and analyzed by the UC Davis Proteomics Core Facility. Protein identification was obtained by using a digestion method for in-gel proteins and analyzed with high resolution mass spectrometry (LC-MS/MS)

where it was determined that the identity of the 70 kDa band was G3BP1 (the his-tag was not verified since the protein database search does not include affinity tags).[29] Furthermore, this result was backed by previous studies that observed the G3BP1 protein near 70 kDa in SDS-PAGE analyses, and the band at 55 kDa was thought to be G3BP1 or another contaminant.[18]

4.2 Pellet #1 from Large Scale Expression #1

pET11a-BL21(DE3)-NHis-G3BP1 was expressed in 1 L of culture according to the method from sections 3.1.3 – 3.1.4, and Figure 7B shows the protein was present in the cells during expression. The pellet from this expression was used for optimizing the large-scale purification protocols that consisted of IMAC and ion exchange purifications to isolate NHis-G3BP1 from the other species in the lysate followed by his-tag cleavage by the TEV protease.

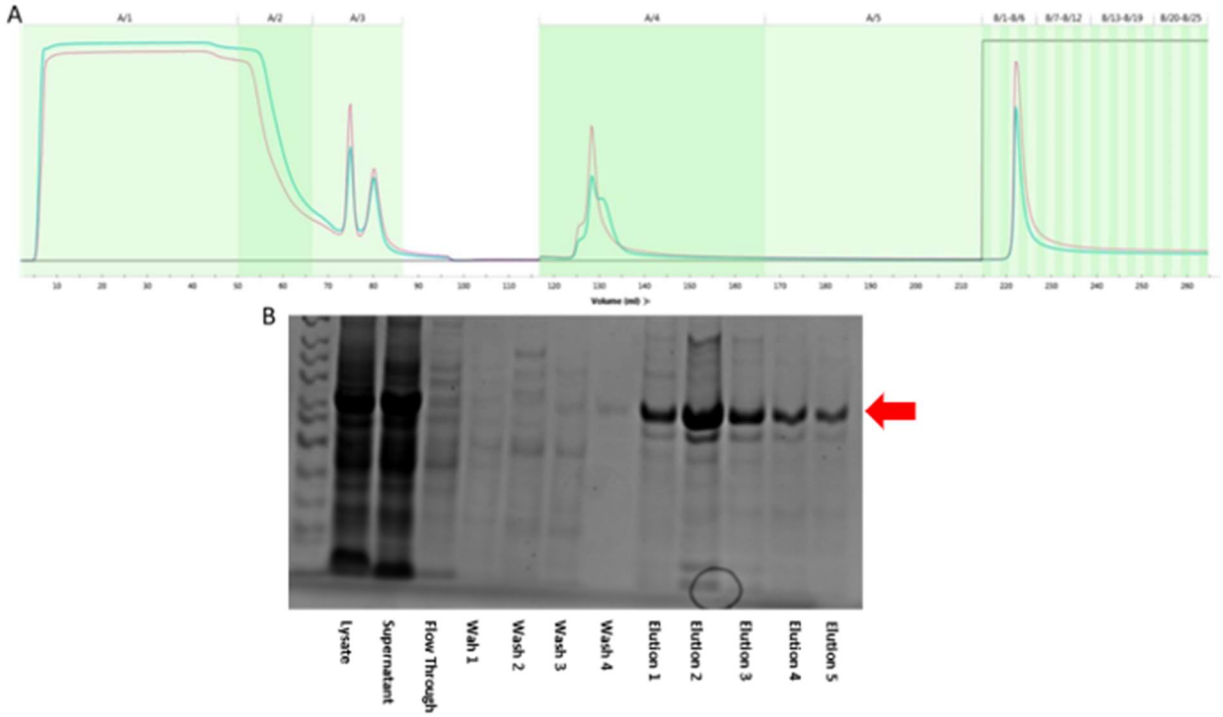

Figure 9: Chromatogram and SDS-PAGE gel from the IMAC purification of NHis-G3BP1. A is the chromatogram of the IMAC purification where the black line is the fraction of imidzole, the red line is the A_{280} measurement, and the green line is the A_{260} measurement as the solution is leaving the Ni^{2+}NTA column. B is the gel of the elution fractions 1 – 5 which were collected in 2 mL aliquots. In addition to NHis-G3BP1 at 70 kDa (red arrow), multiple bands were present in the eluates at weights above and below that correspond to species that are not NHis-G3BP1.

4.2.1 Optimization of IMAC Purification of 1 L pET11a-BL21(DE3)-NHis-G3BP1

The A_{280} measurement and sequence-predicted molar extinction coefficient were used to monitor the protein yield throughout all steps of isolating G3BP1. Using the FPLC, NHis-G3BP1 was purified from the supernatant of a 4.2 g lysed pellet according to the procedures described in section 3.1.6. The supernatant, flow through, wash, and elution fractions were monitored for the presence of nucleic acids and protein by measuring the A_{260} and A_{280}, respectively by UV-vis spectrophotometry attached to the FPLC. The protein concentration can be calculated from the extinction coefficient at 280 nm and the ratio of A_{260}/A_{280} indicates the presence of DNA or RNA. A ratio greater than 0.6 indicates the presence of at least some DNA or RNA in the samples. Since G3BP1 has a nucleic acid binding domain it is important to determine if RNA or DNA is bound to the protein so structural or binding studies of G3BP1 study the protein by itself. SDS-PAGE denatures the protein and removes RNA from the protein which makes it incapable of depicting whether RNA is bound to the protein in solution. However, some nucleic acid binding is expected due to the RNA recognition motif within the G3BP1 structure that binds RNA.

Imidazole is used to outcompete the his-tag of the NHis-G3BP1 protein during the elution step of IMAC. The elution step of the IMAC purification was achieved by running 500 mM imidazole through the FPLC in equilibration buffer, and NHis-G3BP1 was recovered from the column in 10 mL of total sample. To prevent aggregation of the protein from possible concentration-dependent solubility limits, the eluate was diluted twofold in elution buffer before further measurements were taken. The 20 mL sample protein concentration was 36.2 μM. Additionally, all the fractions from the FPLC were analyzed for the efficiency of the purification by SDS-PAGE (Figure 9). There were several bands present in the elution fractions in addition to

the ~70 kDa NHis-G3BP1 band after the IMAC purification, therefore it was necessary for subsequent purification techniques to isolate the pure protein.

4.2.2 Optimization of AEX Purification of NHis-G3BP1

UV-vis can evaluate the presence of nucleic acids (260 nm), protein (280 nm) and light-scattering particles (350 and 600 nm) throughout the entire purification process at specific wavelengths, and SDS-PAGE shows the weights of all species in solution and their relative abundance. To evaluate the conditions that allow NHis-G3BP1 to bind to the AEX column without disrupting its solubility and structure, tests were run with different sodium chloride concentrations in the protein buffer. UV-vis and SDS-PAGE were used to monitor the state of the protein solution before and after dialyzing in suitable buffers for AEX and after collecting the protein from the affinity ion exchange column.

The pH remains the same during the purification, but the sodium chloride concentration needs to be lowered to allow the protein to bind to the column since Cl^- exhibits competitive binding. The decrease in salt can lead to aggregation of the large protein molecule since the kosmotropic nature of sodium chloride minimizes hydrophobic interactions.[30] NHis-G3BP1 has a predicted isoelectric point of 5.71 and is stored in equilibration buffer at pH 7.5 which makes it a suitable candidate for AEX due to the net negative charged on the protein that can bind to the positively charged AEX column. To lower the concentration of sodium chloride, dialysis of the protein from the IMAC purification was performed in 20 mM HEPES (pH 7.5) and followed with UV-vis measurements to assess the effect on solubility. Table 1 shows the absorbance measurements where the values correspond to the presence of RNA (260 nm), protein (280 nm), and aggregation (350 and 600 nm) in the solution. In the absence of sodium chloride, the protein aggregated as indicated by the increase in A_{350} and A_{600} absorbance values, which are attributed

to the scattering of light by aggregated or large particles.[31] Furthermore, the first sample in 20 mM HEPES pH 7.5 was found as a large precipitate a day later in the dialysis tubing and discarded. A second sample from the IMAC purification was then diluted to reduce the protein-protein interactions and dialyzed into 20 mM HEPES and 15 mM sodium chloride (pH 7.5) but was still found to aggregate in the dialysis tubing. After pelleting the aggregates at 20000 x*g* for 20 minutes and removing the supernatant, it was discovered that only 77% of the protein was still soluble and most of the aggregate had been removed from the sample (Table 1).

	IMAC Sample 1	20 mM HEPES	After Spin	Diluted Sample 2	20 mM HEPES + 15 mM NaCl	After Spin
Abs_{260}	.619	2.198	.408	.377	1.743	.319
Abs_{280}	.921	2.159	.598	.583	1.649	.451
Abs_{350}	.043	.953	.006	.007	.818	.022
Abs_{600}	0	.342	-.029	.011	.390	.023

Table 1: The effect of different buffer systems on the absorbance values of NHis-G3BP1 protein in the combined elution fractions after IMAC purification – First, the protein solution was dialyzed in the indicated buffer system and the absorbance values were measured with UV-vis. The protein solution was then spun at 20000 xg for 20 minutes to pellet any light-scattering particles before remeasuring. The wavelengths are selected to evaluate the presence of nucleic acids (260 nm), protein (280 nm) and light-scattering particles (350 and 600 nm).

The dialyzed solution was loaded onto the AEX column that was equilibrated with 20 mM HEPES and 15 mM sodium chloride at pH 7.5. Samples of 2 mL volumes were collected from the column after applying a gradient of sodium chloride from 15 mM – 1 M. Using the UV-vis detector attached to the FPLC, a 280 nm peak was detected in two 2 mL elution fractions, B13 and B14 (Figure 10A). SDS-PAGE results showed bands corresponding to NHis-G3BP1 at 70 and 55 kDa suggesting the purification was successful in recapturing NHis-G3BP1 and reducing some of the contaminants (Figure 10B). However, the purification was not complete as there were additional bands at lower molecular weights.

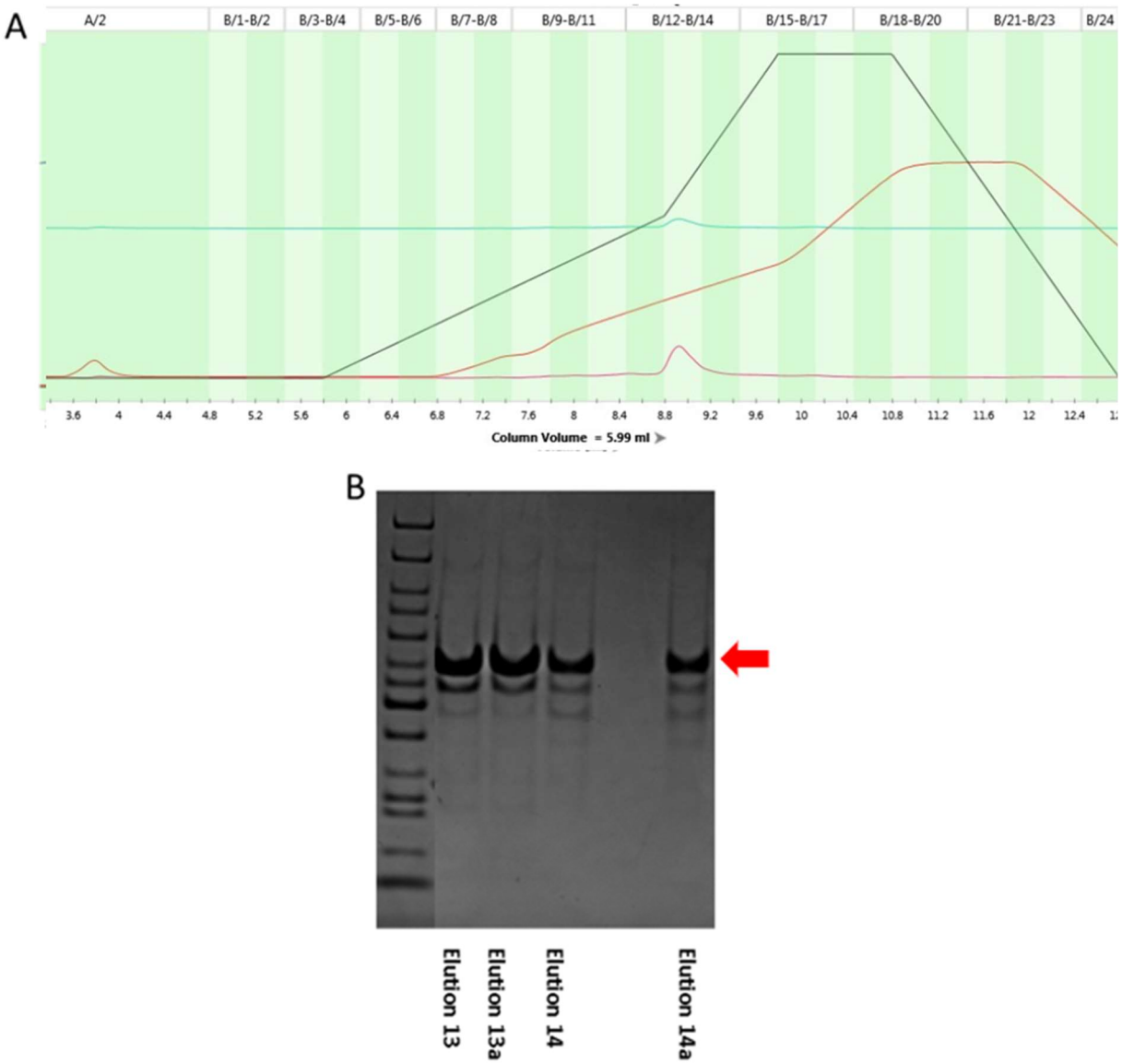

Figure 10: Chromatogram and SDS-PAGE gel of AEX purification of NHis-G3BP1 – A is the chromatogram where the black line is the sodium chloride gradient, the orange line is the conductivity, and the red line is the A_{280} measurement showing the protein concentration in the solution and the blue line is the A_{260} trace of nucleic acids leaving the AEX column. B is the SDS-PAGE gel of samples taken from the 2 mL elution fractions B13 and B14 after AEX purification in duplicate. The red arrow is pointing to the band corresponding to NHis-G3BP1 at 70 kDa. More than one band is present which indicates the purification did not isolate a singular species.

4.2.3 Optimization of TEV Cleavage of NHis-G3BP1

The NHis-G3BP1 that was purified from the AEX column was still his-tagged and TEV was added to the protein solution to cleave the tag to produce G3BP1 without an affinity tag. To calculate the amount of TEV necessary for the cleavage reaction, it was necessary to measure the

amount of NHis-G3BP1 present in the sample using the A_{280} measurement. Additionally, SDS-PAGE can show a decrease in the protein's molecular weight which is observed as a downward shift in the bands corresponding to the protein after the introduction of TEV. A change in weight of 3 kDa is verification that the his-tag has been removed.

The concentration of NHis-G3BP1 was obtained from the A_{280} value after the AEX step (Table 1). The AEX elution fractions were then dialyzed in 20 mM HEPES + 15 mM sodium chloride + 0.5 mM EDTA + 2 mM DTT, and 1 % TEV (mole/mole) was added and allowed to react at 4 °C. Figure 11 shows the samples that were taken at time points of 1, 3, 24 and 48 hours and analyzed by SDS-PAGE to observe the shift in mass due to the his-tag cleavage. The shift is noticeable beginning at the 3-hour mark where there appears to be a mixture of cleaved and uncleaved protein in the form of a smear of bands that correspond to multiple species in the gel sample. By the 48 hour mark the cleavage appears to be complete due to a singular band appearing on the gel with a mass-loss close to the size of the his-tag (3 kDa).

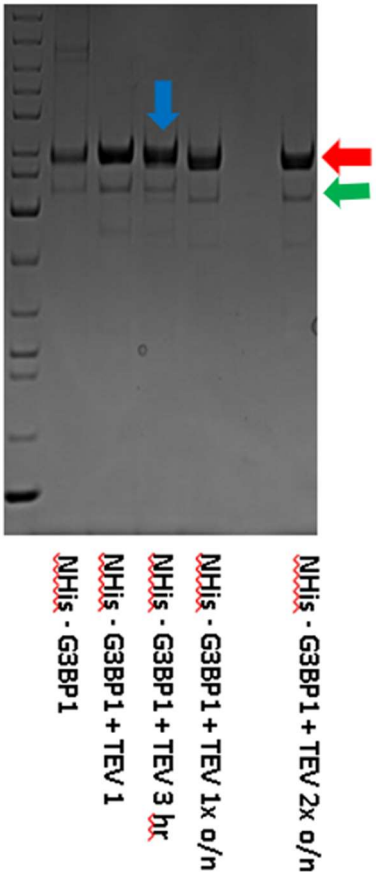

Figure 11: SDS-PAGE gel of the NHis-G3BP1 protein solution before and after TEV is introduced to the solution with samples taken at different time points. The darkest bands are near 70 kDa and correspond to the protein. The observed mass decreases by 3 kDa over reaction time with the protease. The blue arrow shows the beginning of the change in mass as more than one species begins to appear as a smear near 70 kDa, and the red arrow highlights the final contents after 48 hours of incubation where the band is a solid line at 70 kDa which indicates a singular species. The green arrow is pointing at a remaining species at 55 kDa which is thought to be a contaminant.

4.2.4 AEX of G3BP1

The additional AEX was needed to remove the last contaminants that were present after the first AEX where Figure 11 shows an additional band at 55 kDa. The cleaved protein was loaded as a 4 mL solution onto the AEX column of the FPLC with a buffer of 20 mM HEPES and 15 mM sodium chloride (pH 7.5) used to equilibrate the column. A 15 mM – 1 M gradient of sodium chloride was used to elute the protein and separate it from other species in solution. A 280 nm peak was observed in the chromatogram and 2 mL fractions (B10 – B12) were collected (Figure 12A). The eluates' absorbances at 260, 280, 350 and 600 nm were measured (Figure 12C) and compared to the values before the TEV cleavage in Table 1 to assess the nucleic acid,

protein, and insoluble particle content, respectively. The flow through, wash and elution fractions were then evaluated with SDS-PAGE for the purity of the solution (Figure 12B). The absorbance values decreased to less than 15 % of the values before ion exchange and faint bands were present in the elution and flow through fractions meaning that most of the protein was lost throughout the purification step as an aggregate or it never bound to the column and was diluted to the point of being unobservable in the gel (Figure 12B). To figure out how to run AEX without losing most of the protein in the process, a new batch of protein and condition tests were necessary.

A

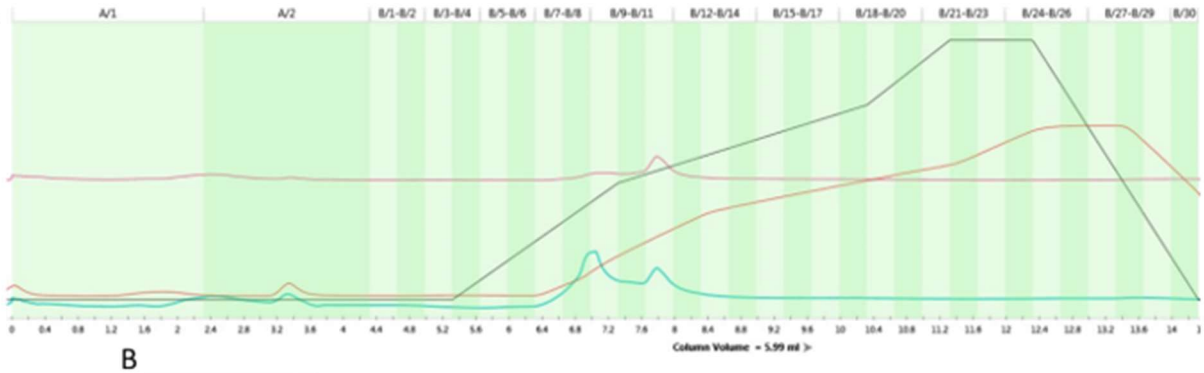

B

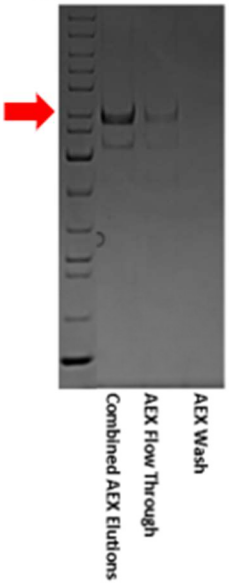

C

	Sample Before Cleavage	Elution B10	Elution B11	Elution B12
Abs_{260}	.098	.016	.016	.012
Abs_{280}	.117	.006	.016	.006
Abs_{350}	0	0	0	0
Abs_{600}	0	0	0	0

Figure 12: Chromatogram of AEX purification of G3BP1 with accompanying SDS-PAGE gel and absorbance measurements corresponding to the species that came off the FPLC column – A is the chromatogram of the AEX purification where the black line is the sodium chloride gradient, the orange line is the conductivity of the solution, the red line is the A_{280} measurement to

monitor the protein content and the blue line is the A_{260} measurement to monitor the nucleic acid content of the solution coming off the FPLC column. B is the SDS-PAGE gel of the elution, flow through and wash fractions that were collected from the FPLC where the red arrow is pointing to the G3BP1 species molecular weight (70 kDa). There is protein in the elution, but the band is faintly there in the flow through and completely gone in the wash fraction. C is the table of absorbance measurements of the G3BP1 sample that was taken before adding to the AEX column and the elution fractions that were collected after running on the FPLC.

4.3 Pellet #1 from Expression #2

Figure 7B shows the expression of 2 L of pET11a-BL21(DE3)-NHis-G3BP1 where 1 L aliquots were pelleted according to the method outlined in sections 3.1.3 – 3.1.4, and the cells were frozen for future purifications of G3BP1.

4.3.1 IMAC Purification of pET11a-BL21(DE3)-NHis-G3BP1

A 3.3 g pellet was lysed and the NHis-G3BP1 protein was purified as described in section 3.1.6 with two changes: 500 mM sodium chloride was used in the lysis, equilibration, and elution buffers to account for the susceptibility of the protein to aggregate under conditions of low salt, and a gradient of 0-500 mM imidazole was used in the elution step to separate contaminants from the protein as well as dilute the final concentration. Figure 13A shows the resulting chromatogram of the IMAC purification where a large peak was detected during the elution gradient step. The elution fractions were combined and dialyzed in equilibration buffer (with 500 mM sodium chloride) at 4 ℃ overnight to remove the imidazole from the protein solution. Figure 13B shows the SDS-PAGE gel where the combined elution fractions show a large band at 70 kDa corresponding to NHis-G3BP1, but there are many other bands present as well, likely arising from impurities or proteolytic cleavage of the G3BP1 protein.

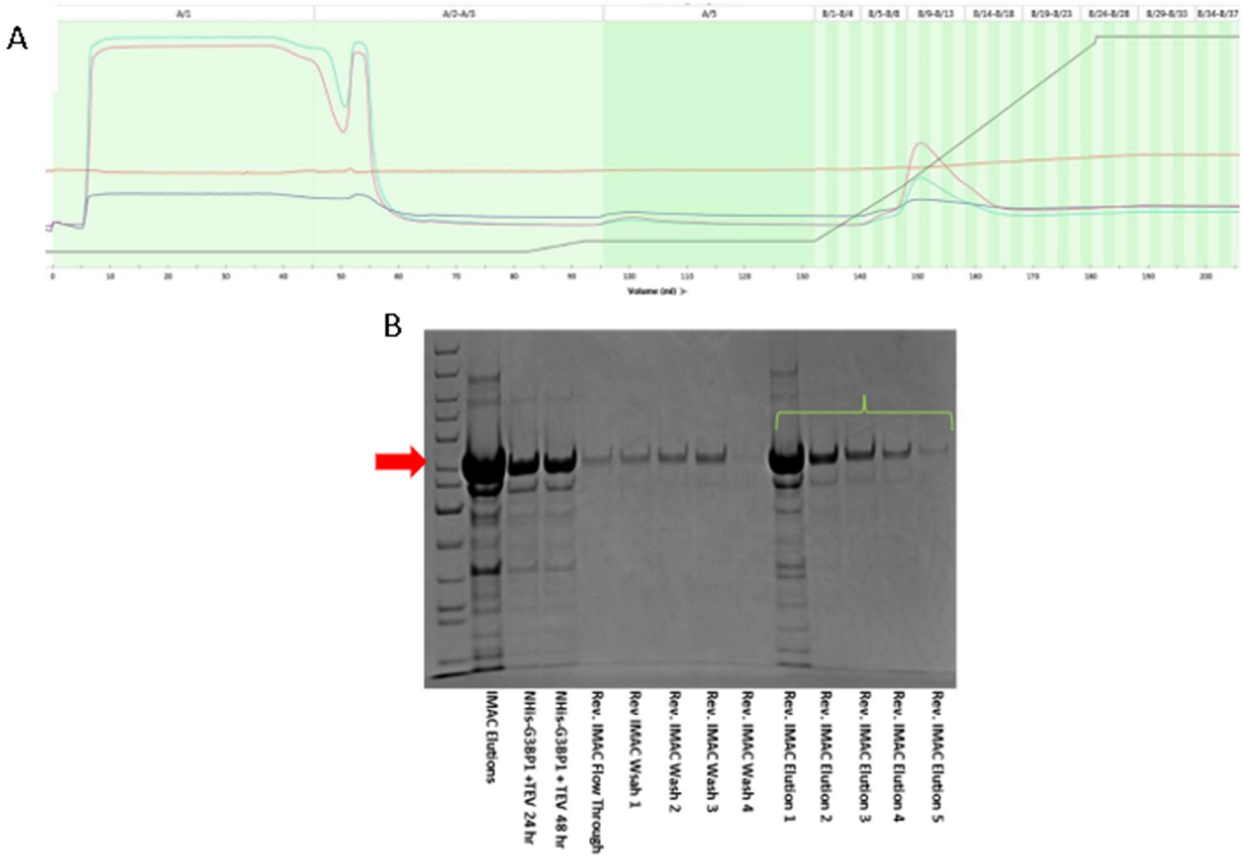

Figure 13: IMAC chromatogram and SDS-PAGE gel of G3BP1 collections throughout the IMAC, TEV cleavage, and reverse IMAC steps – A is the chromatogram of the IMAC purification where the black line shows the gradient of imidazole and the red line and blue line are the A_{280} and A_{260} measurements, respectively, that are tracked for the protein and nucleic acid content of the solution coming off the column. B is the gel containing samples of the elution fractions combined from the IMAC purification; timepoints of the combined eluate with the TEV protease at 24 and 48 hours of reaction time; and the flow through, wash and elution fractions collected off the Ni^{2+}-NTA column during reverse IMAC. The red arrow is at 70 kDa where the band corresponding to NHis-G3BP1 species. This species is present in all steps even after the addition of TEV which indicates the TEV cleavage did not occur. Additionally, the elution fractions of the reverse IMAC (green bracket) contain most of the protein which were collected after the application of imidazole to remove the his-tagged protein which supports the conclusion that the TEV cleavage reaction did not work.

4.3.2 TEV Cleavage of Elution Fractions and Reverse IMAC Purification

The next step was adding TEV to the elution fractions to cleave the his-tag before purifying with AEX. This can be verified with SDS-PAGE where the decrease in protein mass after adding TEV shows the cleavage. Prior attempts at cleaving the tag occurred between two AEX purifications, but protein was lost under the low salt conditions with 15 mM sodium chloride that was required by ion exchange. Therefore, AEX purification was delayed until after

TEV cleavage as it presented unfavorable buffer conditions for the solubility of the protein and would only be performed once.

IMAC elution fractions adding up to 17 mL NHis-G3BP1 were obtained after dialysis and 77 μM was the approximate concentration based on the A_{280} value, however there was significant light scattering in the longer wavelengths (350 and 600 nm). One reason for the presence of light scattering is that the concentration of the protein in the buffer exceeded the solubility limit and produced insoluble particulate that was observed by scattered light intensity at longer wavelengths.[32] To reduce the concentration of protein in solution and remove any insoluble particulates, the sample was diluted twofold with dialysis buffer and pelleted at 20000 x*g* for 20 minutes and the supernatant was removed. The final concentration was near 31.5 μM which is a decrease more than that of the dilution factor meaning some of the protein from the elution was lost during dialysis or the light scattering from aggregate protein increased the baseline of the initial A_{280} measurement. After spinning down the particulate matter, the light scattering was reduced, and the insoluble species was successfully removed from solution. Afterward, 1% TEV (mole/mole) was added to the supernatant, and it was placed within dialysis tubing and dialyzed with fresh dialysis buffer at 4 ℃ to remove more imidazole from the buffer that was present in the elution step of the IMAC purification. Another 1 % (mole/mole) TEV was added to the dialysis tubing 24 hours later and was allowed to react for an additional 24 hours at 4 ℃ to enhance the likelihood of affinity tag cleavage.

4.3.3 Reverse IMAC of TEV and NHis-G3BP1

An additional IMAC purification termed reverse IMAC would now be performed on a gravity column after the initial IMAC purification and TEV cleavage. In traditional IMAC, the protein binds to the column with its his-tag, but in reverse IMAC purification the protein should

not bind to the column since the affinity tag is not present and therefore has minimal binding capacity for the Ni^{2+}-NTA column. Therefore, it is expected that the protein should be collected in the flow through and wash fractions while the uncleaved protein and remaining his-tags should be found in the elution fractions. This has the effect of isolating the two protein species (G3BP1 and uncleaved NHis-G3BP1) and removing the his-tag from the cleaved protein solution.

Reverse IMAC was performed on the newly cleaved sample from dialysis on a Ni^{2+}-NTA gravity column. The dialysis buffer from the TEV cleavage reaction was used to equilibrate the column followed by 20 mM imidazole wash and 500 mM Imidazole elution buffers. The flow through, wash, and elution fractions were collected and analyzed with SDS-PAGE (Figure 13B). The results indicated that the cleavage was not complete due to the large band at 70 kDa in the elution fractions that was significantly more prevalent than the bands of the flow through and wash where the G3BP1 species was expected if the TEV cleavage was successful. Additionally, there was no shift in mass from the fractions collected before and after the addition of TEV. To improve the results of his-tag cleavage from the NHis-G3BP1, the elution fractions were pooled together and followed by another addition of 2% TEV (mole/mole) before the sample was placed back in the dialysis buffer for 14 days at 4 ℃.

4.3.4 AEX of G3BP1

Figure 14B shows contaminants in the protein solution collected from the reverse IMAC purification according to SDS-PAGE, and AEX was used to separate these additional species from G3BP1. The dialyzed sample was removed and placed in a new dialysis buffer that was appropriate for AEX, 20 mM HEPES pH 7.0, and stored overnight at 4 ℃. This was loaded onto the AEX column of the FPLC equilibrated with the dialysis buffer containing 20 mM HEPES

and 20 mM sodium chloride, pH 7.0. The sample was eluted with a gradient of 20 mM – 1.0 M sodium chloride, and the corresponding chromatogram in Figure 14A shows no peak in any of the fractions. The SDS-PAGE gel shows no observable protein in the collected wash or elution fractions, but it was present before loading onto the column which indicates that the protein was lost at some point during the purification step.

Ultimately, the protein was successfully captured from the cell lysate using IMAC purification in buffers containing high salt (500 mM sodium chloride). However, some contaminating species remained that required additional purification steps, and some aggregation occurred that led to some protein loss. The initial cleavage of the his-tag was mostly unsuccessful in the high salt buffer after two 1 % additions of TEV and 48 hours of reaction time. This was verified by the SDS-PAGE gel where the protein remained on the Ni^{2+} affinity column until the elution step which indicated the his-tag was still attached to G3BP1 and able to bind to the column (Figure 13B). The loss of TEV activity was likely caused by the increase in sodium chloride during the reaction as TEV has been shown to lose activity at sodium chloride concentrations above 200 mM.[19] After dialyzing the protein into low salt AEX buffer conditions and running the ion exchange purification, the protein was not observed in the accompanying FPLC chromatogram or the SDS-PAGE gel of the elution fractions (Figure 14). The low salt buffer conditions potentially led to protein insolubilization and the complete loss of the sample. A new pellet of cells containing NHis-G3BP1 would need to be lysed and purified to ameliorate these difficulties and determine the correct conditions to isolate and cleave the G3BP1 protein.

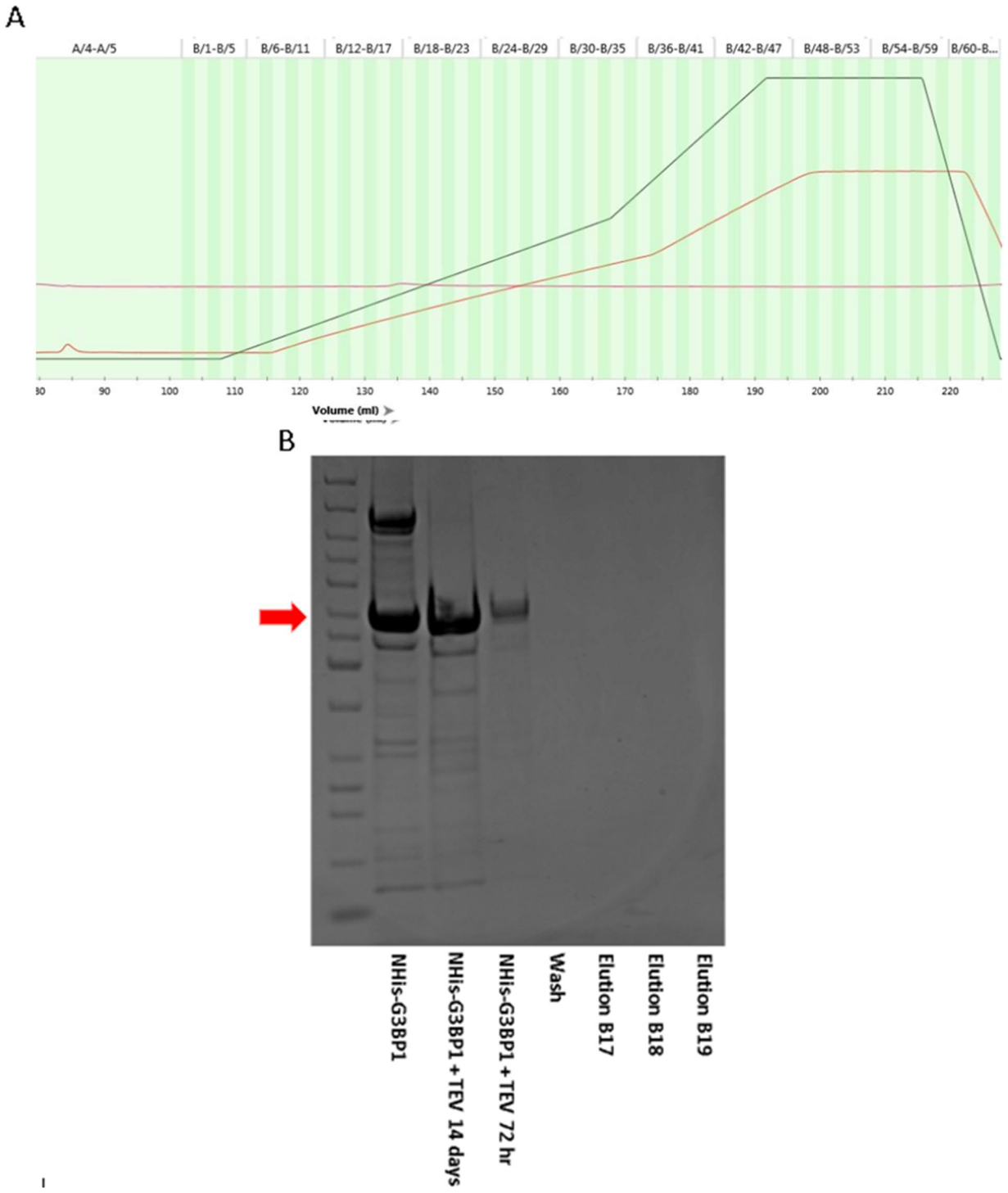

Figure 14: AEX purification and TEV cleavage of the NHis-G3BP1 protein solution before and after TEV cleavage reaction – A is the chromatogram of the AEX purification step where the black line is the sodium chloride gradient, the orange line is the conductivity of the solution, and the red line is the A_{280} trace monitoring the presence of protein that is leaving the FPLC from the AEX column. B is the SDS-PAGE gel of the NHis-G3BP1 protein solution before and after TEV is introduced and reacted for multiple time points along with the wash and elution fractions from the AEX purification. There is nothing observable in the AEX purification collections meaning G3BP1 was not collected.The red arrow is pointing at the G3BP1 protein before and after cleavage.

4.4 Pellet #2 of Expression #2

It was necessary to purify a new pellet from the previous growth to test more purification conditions. Less sodium chloride was used in the buffers to increase TEV activity in the cleavage reaction.[19] Also, 10 mM sodium chloride was added in the AEX buffers since the absence of salt led to a loss of protein throughout the ion exchange technique.

4.4.1 IMAC Purification of pET11a-BL21(DE3)-NHis-G3BP1

A 3.8 g pellet was lysed in lysis buffer and purified on the FPLC IMAC column in NHis-G3BP1 IMAC equilibration buffer as described in section 3.6 and the chromatogram in Figure 15A revealed a large peak in the elution step. The elution fractions were examined with SDS-PAGE to observe the efficiency of the purification regarding the number of bands that correspond to multiple species in solution with NHis-G3BP1 (Figure 15B). Like previous IMAC purifications, the resulting gel showed multiple species along with NHis-G3BP1. The elution fractions were combined and dialyzed into the equilibration buffer at 4 ℃ overnight to remove imidazole for TEV cleavage.

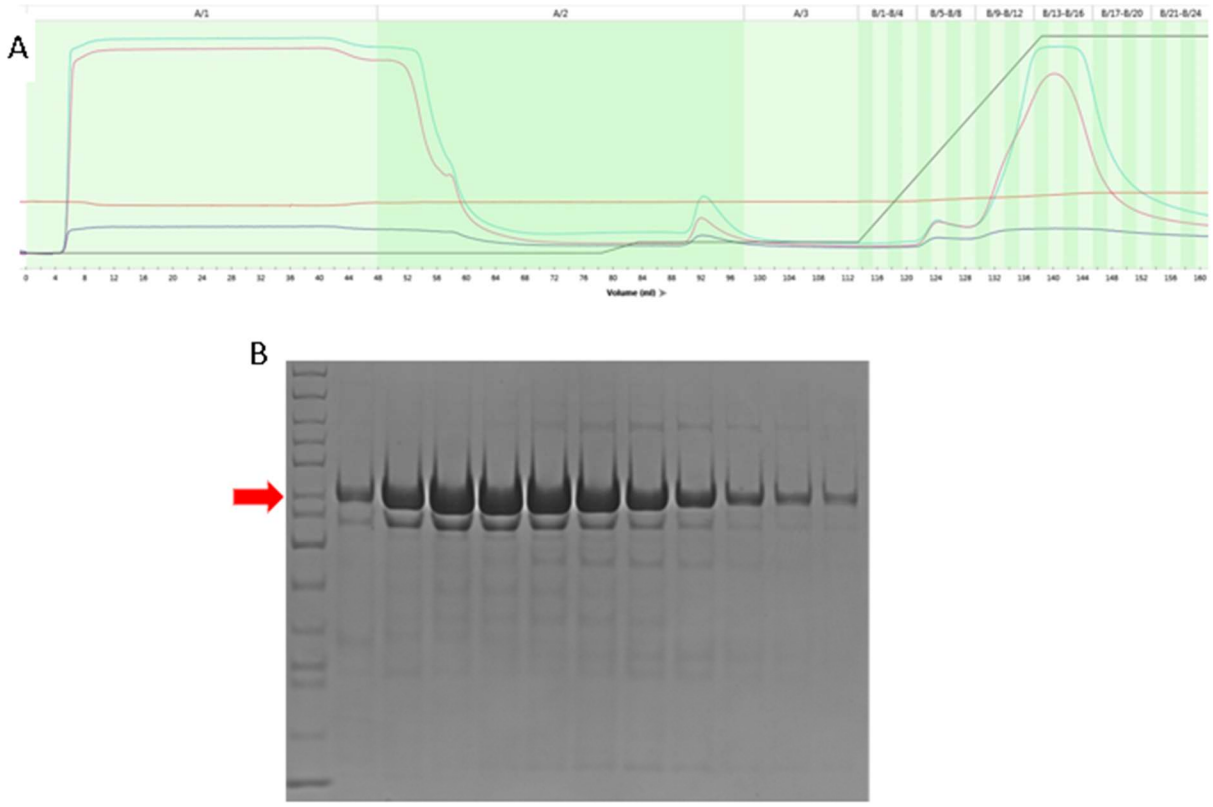

Figure 15: Chromatogram and SDS-PAGE gel of the IMAC purification of NHis-G3BP1 – A is the chromatogram of the IMAC purification of NHis-G3BP1 where the black line is the imidzole concentration gradient, the blue line is the A_{280} measurement and the red line is the A_{260} measurement where the two lines are used to monitor the protein and nucleic acid content of the solution, respectively, as it comes off the FPLC column. B is the SDS-PAGE gel of the eleven 2 mL elution fractions that were collected from the FPLC column.

4.4.2 TEV Cleavage of Elution Fractions

After dialysis, the concentration of 20 mL of protein eluate was measured to determine the amount of TEV to add. Initially the A_{280} value equated to 142 µM protein, but there was a visible white precipitate that formed in the dialysis tubing and the light scattering at wavelengths of 350 and 600 nm was substantial. Since G3BP1 is an RNA-binding protein that forms complexes with other biomolecules, it is possible that RNase can be used to remove the RNA species that were part of the complex that led to precipitation. To test this, 10 µg/mL RNase was added to the dialysis tubing which was placed into 1 L fresh equilibration buffer at 4 °C for 1 hour. The sample was removed from the tubing, and the precipitate was gone. This freshly dialyzed sample was pelleted at 15000 x*g* for 10 minutes to remove any remaining aggregates

from solution. Before taking new UV-vis measurements, the sample was diluted fivefold with equilibration buffer to reduce protein-protein interactions that can lead to aggregation from the concentration being above the solubility threshold of G3BP1 in the buffer.[32] The A_{280} measurements showed that 100 mL of sample contained 30 μM protein. A 3.6% TEV aliquot (mole/mole) was added to the sample and dialyzed in equilibration buffer overnight at 4 °C. The TEV cleavage reaction exhibits increased activity at room temperature, so the dialyzed sample was allowed to react at room temperature for an additional two hours after removing from the 4 °C environment to produce more his-tag cleavage from G3BP1.[19]

4.4.3 Reverse IMAC of TEV and NHis-G3BP1

If the TEV cleavage reaction was successful, then the his-tag was cleaved from G3BP1, and the protein should not bind to the Ni^{2+}-NTA resin during reverse IMAC purification. Previous attempts to cleave the tag were unsuccessful, so small-scale reverse IMAC tests were performed to evaluate the binding affinity of the protein before purifying the rest of the protein solution. These small-scale tests were done with 250 μL Ni^{2+}NTA resin and 500 μL protein solution in a microcentrifuge tube where the column was incubated with the sample and spun at 2000 x*g* for two minutes while collecting the supernatant after each spin. The flow through, wash and elution supernatants were monitored by their A_{280} values to assess the presence of protein. Most of the protein was found in the flow through and wash steps suggesting that TEV was effective in cleaving the affinity tag as it was unable to bind to the column in the absence of imidazole. Therefore, the remaining 100 mL of protein solution was added to a Ni^{2+}NTA gravity column for reverse IMAC purification, and the flow through, wash and elution fractions were collected separately.

4.4.4 AEX of G3BP1

AEX was performed on the flow through fractions from the reverse IMAC purification to remove more contaminants from the protein solution that were visible in the previous SDS-PAGE gel (Figure 15B). The combined flow through fractions were spin-concentrated to 60 mL to make fitting into the dialysis tubing easier. The 60 mL of protein solution were then dialyzed in 20 mM HEPES, 10 mM sodium chloride, 1 mM DTT, pH 7.6 at 4 ℃ for 2 days to prepare it for AEX. The concentration of the 60 mL protein solution before addition to the AEX column was 26 µM as determined by the A_{280}. The column was equilibrated with 20 mM HEPES (pH 7.5), and the protein was eluted with a gradient of 0 – 1 M sodium chloride in eleven 2 mL fractions (Figure 16A). Figure 16B of the SDS-PAGE gel shows the typical G3BP1 band near 70 kDa and the presence of multiple bands that were not apparent after the initial IMAC purification (Figure 15B) at weights below 55 kDa. The most prevalent band is around 45 kDa which is thought to be a product of proteolysis due to the mass being smaller than the full length G3BP1. The protein was not able to be recovered for further studies, and a new batch of cell pellets would need to be lysed for more attempts at producing purified G3BP1.

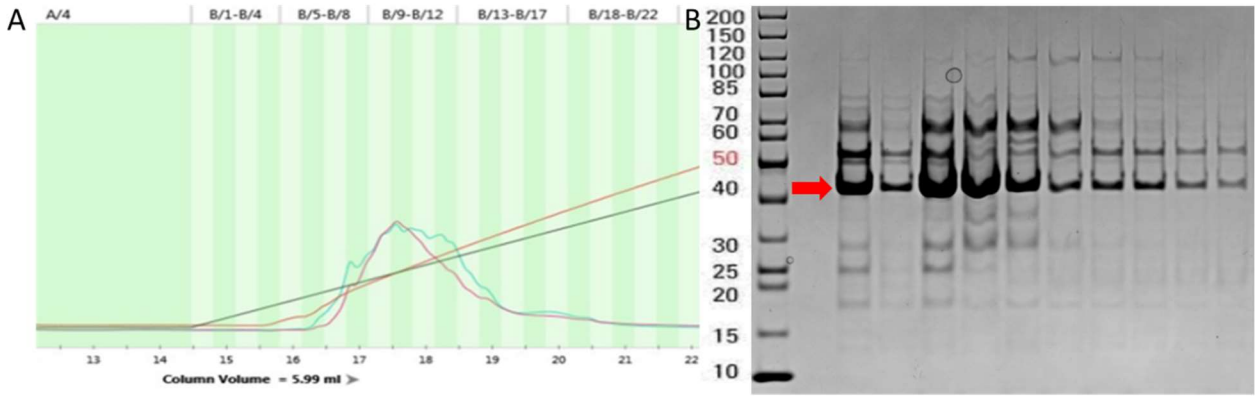

Figure 16: Chromatogram and SDS-PAGE gel of G3BP1 elution - A is the chromatogram of the elution portion of the AEX purification of G3BP1 where the black trace is the sodium chloride gradient, the orange trace is the conductivity of the solution, the red trace is the A_{280} measurement and the green trace is the A_{260} measurement tracking the protein and nucleic acid content of the solution comingoff the FPLC column, respectively. B is the SDS-PAGE gel of the 2 mL elution fractions B5 – B14 where the red arrow is pointing to the new species at 45 kDa that is the most prevalent band in each fraction. This is 12 kDa smaller than the typical observed mass of G3BP1 near 67 kDa and is a potential result of proteolysis.

4.5 Pellet #1 of Expression #3

Cultures of 4 L pET11a-BL21(DE3)-NHis-G3BP1 were grown and expressed, and 1 L aliquots were pelleted and stored according to the method outlined in 3.1.3 – 3.1.4. These pellets were used in future attempts to isolate G3BP1 from the lysate for experimental studies.

4.5.1 IMAC Purification of pET11a-BL21(DE3)-NHis-G3BP1

A 3 g pellet was lysed, and the supernatant was applied to the IMAC purification column of the FPLC as described in section 3.1.6. Proteolysis was a potential cause of the many species in the SDS-PAGE gel in Figure 16B that was obtained after the most recent AEX purification. Therefore, the NHis-G3BP1 IMAC equilibration buffer was supplemented with 0.1 mM PMSF for its ability to inhibit serine proteases. There was an obvious A_{280} peak in the chromatogram during the elution step and the SDS-PAGE gel showed a band corresponding to NHis-G3BP1 (Figure 17). The elutions were pooled and dialyzed at 4 ℃ overnight into fresh equilibration buffer with 20 mM BME, 1 mM EDTA and lowered salt (150 mM sodium chloride) where the salt change was implemented to increase the activity of TEV cleavage according to previous publications on ideal TEV activity.[19]

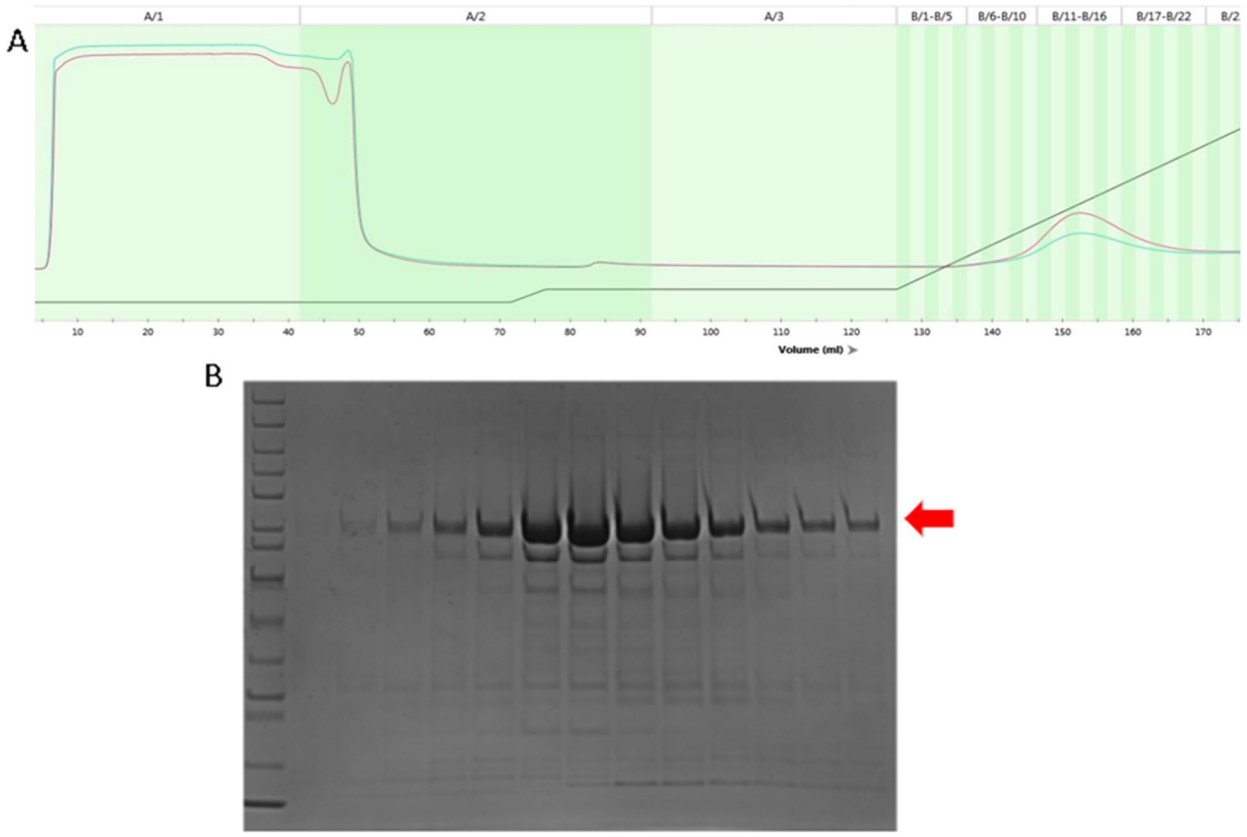

Figure 27:Chromatogram and gel of IMAC purification of the NHis-G3BP1 protein – A is the chromatogram of the IMAC purification where the black line corresponds to the imidazole gradient and the red and green lines correspond to the A_{280} and A_{260} measurements throughout the run. B is a SDS-PAGE gel of the 2 mL elution fractions B6 – B16. The darkest bands indicated by the red arrow are at the observed molecular weight of NHis-G3BP1.

4.5.2 TEV Cleavage of Elution Fractions

A_{280} measurements were taken of the eluate to assess the amount of NHis-G3BP1 which is necessary to know how much TEV to add for the cleavage reaction. From dialysis, the protein solution had a volume of 32 mL with a concentration of 25.7 µM. To cleave the his-tag from the NHis-G3BP1 protein, 2% (mole/mole) TEV was added to the sample and the dialysis tubing was placed into 1 L fresh dialysis buffer at 4 °C for 48 hours to remove more sodium chloride and imidazole from the sample.

4.5.3 Reverse IMAC of TEV and NHis-G3BP1

The sample containing NHis-G3BP1 and TEV was removed from dialysis and loaded on an equilibrated Ni^{2+}NTA gravity column where the dialysis buffer was used as equilibration

buffer and the wash buffer. The elution step used dialysis buffer supplemented with 500 mM imidazole to remove the remaining species bound to the Ni^{2+}-NTA resin. Flow through, wash and elution fractions were monitored by UV-vis for the presence of protein in addition to SDS-PAGE. From the gel image, it was apparent that most of the protein was found in the flow through and wash fractions. This was expected after successful TEV cleavage since the his-tag is removed from the G3BP1 protein resulting in a much lower affinity for the Ni^{2+}NTA column. Also, there was an observable downward shift in their mass from 70 kDa to 67 kDa when compared to the lysate and supernatant fractions before the IMAC purification indicating the loss of the 3 kDa his-tag (Figure 18A). The flow through and wash fractions were then pooled and placed into a dialysis buffer of 20 mM HEPES, 1 mM DTT (pH 7.5) at 4 °C for 2 days to prepare for AEX.

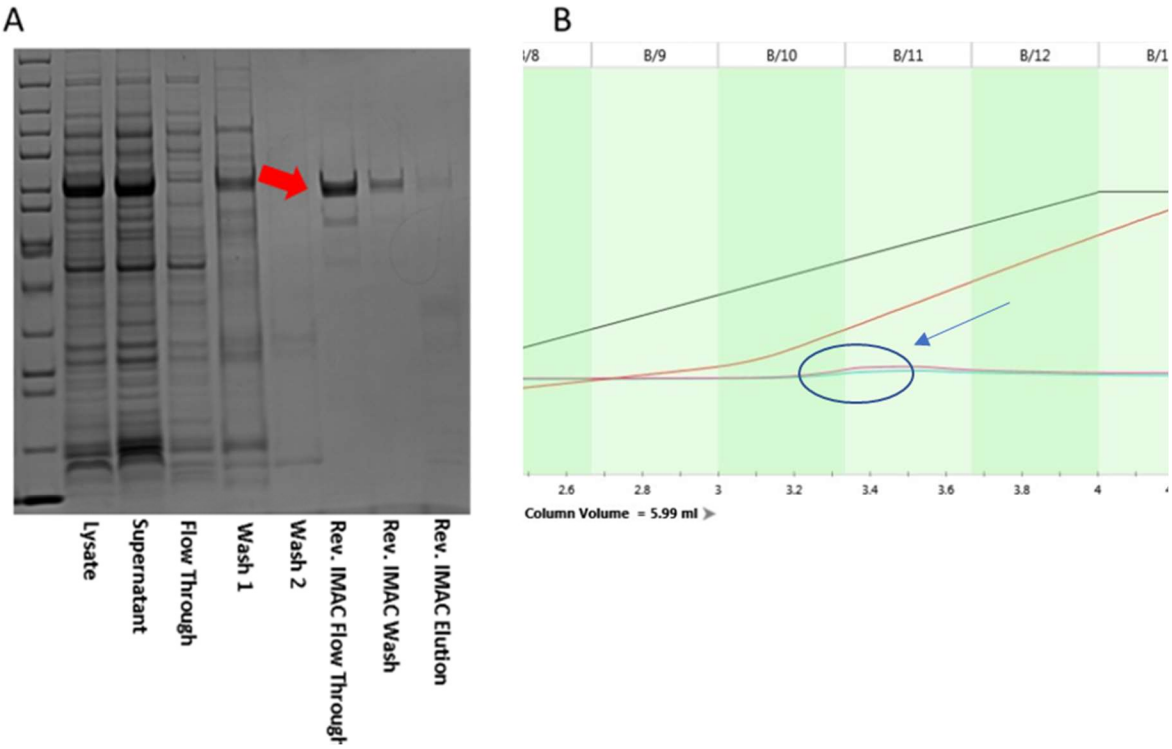

Figure 38: Gel of IMAC and Reverse IMAC purification fractions and chromatogram from AEX – A is the SDS-PAGE gel of the lysate, supernatant, flow through and wash fractions from the IMAC purification where the darkest bands correspond to the NHis-G3BP1 protein throughout the procedure near 70 kDa. The reverse IMAC fractions show a decrease in the apparent molecular mass of G3BP1 after TEV cleavage compared to the IMAC fractions. This shift is close to the weight of the his-tag (3

kDa) indicated by the slanted red arrow. Most of the protein is found in the flow through and wash fractions near 67 kDa. B is the partial chromatogram of the AEX purification focused on the elution fractions where the only discernible peak is circled. The black line corresponds to the sodium chloride gradient and the red and green lines correspond to the A_{260} and A_{280} values, respectively.

4.5.4 AEX of G3BP1

After TEV cleavage of the his-tag, ion exchange chromatography was performed to remove any remaining contaminants from the protein solution. The newly cleaved sample was taken out of dialysis and the AEX column was equilibrated with fresh dialysis buffer to reduce the salt concentration for the enhancement of protein binding to the column. The protein was loaded onto the column and eluted with a gradient of 0 – 2 M sodium chloride. Unfortunately, the chromatogram in Figure 18B revealed only a small peak that is a sign the purification again did not work and the elutions were discarded.

If proteolysis had taken place, like previously thought, protein should show up in the chromatogram and SDS-PAGE gel at some point during the purification process in smaller lengths than the full G3BP1 protein. However, no protein was observed, and the most likely case would be that no species entered the column due to an issue such as aggregation. It is more than likely that the salt concentration in the AEX buffer or column is the cause of this issue since the protein seems to behave until the ion exchange step. Either way, new protein would need to be purified for more inquiries into the proper conditions for complete G3BP1 isolation from all contaminants.

4.6 Pellet #2 of Expression #3

A new cell pellet containing NHis-G3BP1 was prepared for isolation of G3BP1 while implementing the findings of previous attempts. IMAC purification was followed by TEV cleavage where sodium chloride concentrations above 200 mM seemed to minimize TEV

cleavage activity. Buffers during this reaction would consist of sodium chloride concentrations less than 200 mM. To isolate NHis-G3BP1 from G3BP1 after the cleavage reaction, reverse IMAC would be implemented, and this would be followed by AEX to remove the remaining species from the protein solution.

4.6.1 IMAC Purification of pET11a-BL21(DE3)-NHis-G3BP1

A 3 g pellet was purified on the FPLC using lysis and NHis-G3BP1 IMAC equilibration buffer as described in section 3.1.6. There was an obvious A_{280} peak in the chromatogram during the elution step and the SDS-PAGE gel showed a band corresponding to NHis-G3BP1 (Figure 19). The elution fractions were combined and dialyzed in equilibration buffer with a lower salt concentration (100 mM sodium chloride) to increase the activity of the TEV cleavage. The dialysis was placed at 4 ℃ overnight.

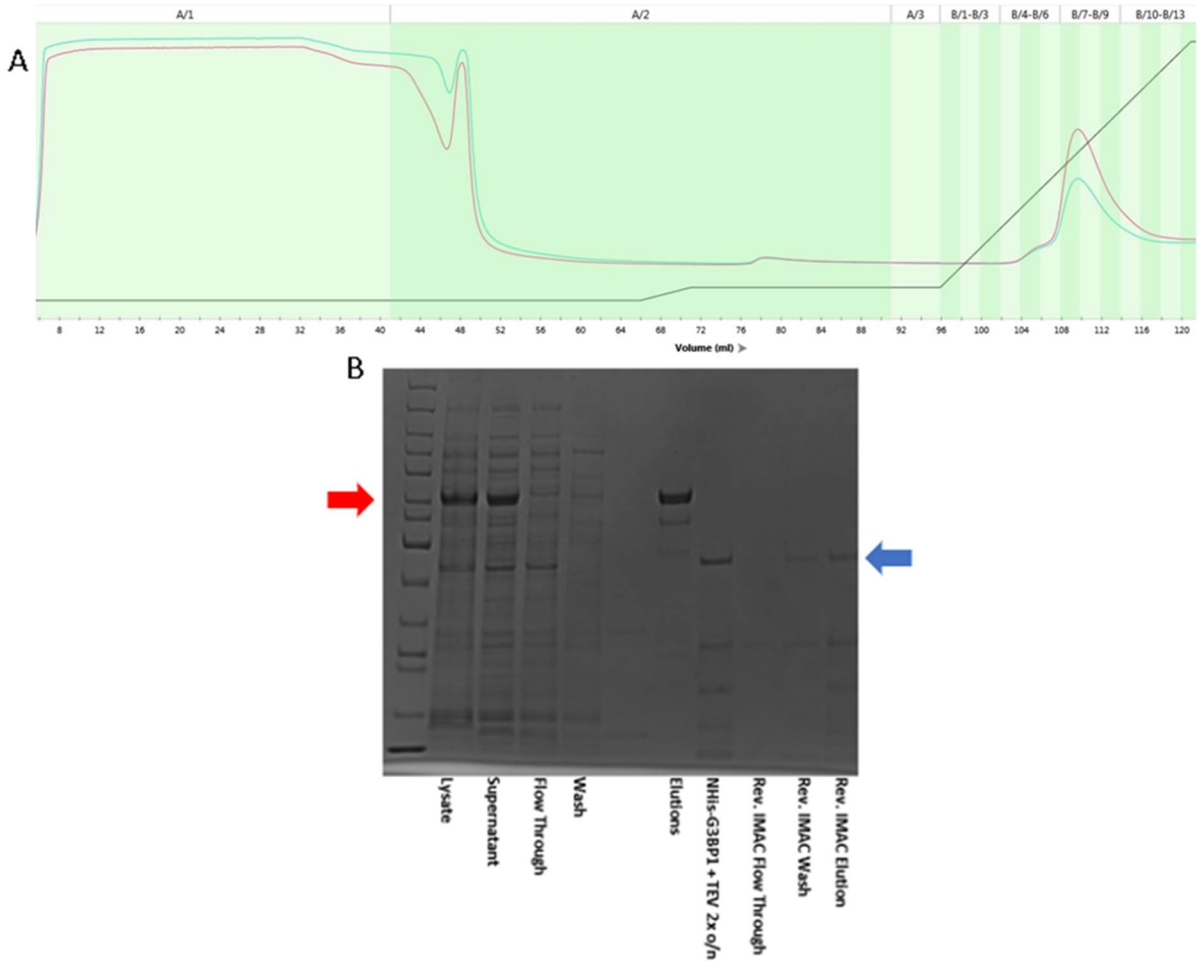

Figure 19: IMAC and reverse IMAC purification of NHis-G3BP1 and G3BP1 – A is the IMAC chromatogram of the NHis-G3BP1 after the lysis step where the black line is the imidazole gradient and the red and blue lines are the A_{280} and A_{260} UV-vis traces monitoring the presence of protein and nucleic acids, respectively, as the solution is collected from the Ni^{2+}-NTA column. B is the SDS-PAGE gel of the IMAC puriication and reverse IMAC purification where the band at 70 kDa (red arrow) corresponds to NHis-G3BP1 before TEV cleavage and the band near 40 kDa is an unintended result after TEV cleavage where the G3BP1 is no longer observed at its expected molecular weight location at 67 kDa.

4.6.2 TEV Cleavage of Elution Fractions

The following day, the A_{280} was measured of the sample for concentration estimates which amounted to 20 mL of 41.7 µM protein. 2% (mole/mole) TEV was added to the dialysis tubing and the mixture was placed in fresh dialysis buffer at 4 °C for 2 days to allow for the cleavage reaction to take place.

4.6.3 Reverse IMAC of TEV and NHis-G3BP1

The sample was removed from dialysis and loaded over a Ni^{2+}-NTA gravity column to separate the cleaved G3BP1 protein from any species that bound to the Ni^{2+}-NTA resin. The column was equilibrated with dialysis buffer and washed with this buffer as well. Elution occurred with an additional 500 mM imidazole in freshly prepared solution to remove any remaining species bound to the column. Flow through, wash and elution fractions were monitored by UV-vis to account for the presence of protein, and the elution fraction appeared to have the most protein by its a_{280} measurement. Unfortunately, the SDS-PAGE gel showed that the species that was captured before and after the reverse IMAC purification was not any expected form of G3BP1 and was most prevalent near 45 kDa (Figure 19B). This is indicative of aggregation or proteolysis based on the observations during the AEX purification in section 4.4.4. Proteolysis and the lack of salt in the dialysis and reverse IMAC buffers were suspected as being the cause for the appearance of this species at 45 kDa. As a result, a new pellet was required to initiate a new iteration of purification. It should be noted in future inquiries that the G3BP1 sequence does not have an endogenous TEV recognition site meaning that the protein is not susceptible to further proteolysis after the addition of TEV during affinity tag removal. Additionally, any degradation must have an external origin as the BL21(DE3) strain is engineered to exclude common proteases.

4.7 Pellet #3 of Expression #3

A new pellet was prepared to isolate G3BP1 according to sections 3.1.6 – 3.1.8. The TEV cleavage step was performed with 100 mM sodium chloride for increased activity and AEX was performed to remove as many contaminants as possible from the protein solution.[19]

4.7.1 IMAC Purification of pET11a-BL21(De3)-NHis-G3BP1

A new 3 g pellet was lysed and purified on the IMAC column of the FPLC according to section 3.1.6. There was an obvious A_{280} peak in the chromatogram during the elution step and the SDS-PAGE gel showed a band corresponding to NHis-G3BP1 (Figure 20). Again, the NHis-G3BP1 IMAC equilibration buffer was supplemented with 0.1 mM PMSF to rule out proteolysis as a potential cause of the apparent degradation of the protein during the TEV cleavage and reverse IMAC steps. The elution fractions were pooled and dialyzed into equilibration buffer with a lower salt concentration (100 mM sodium chloride) per the guidelines of TEV activity and placed at 4 ℃ overnight.[19]

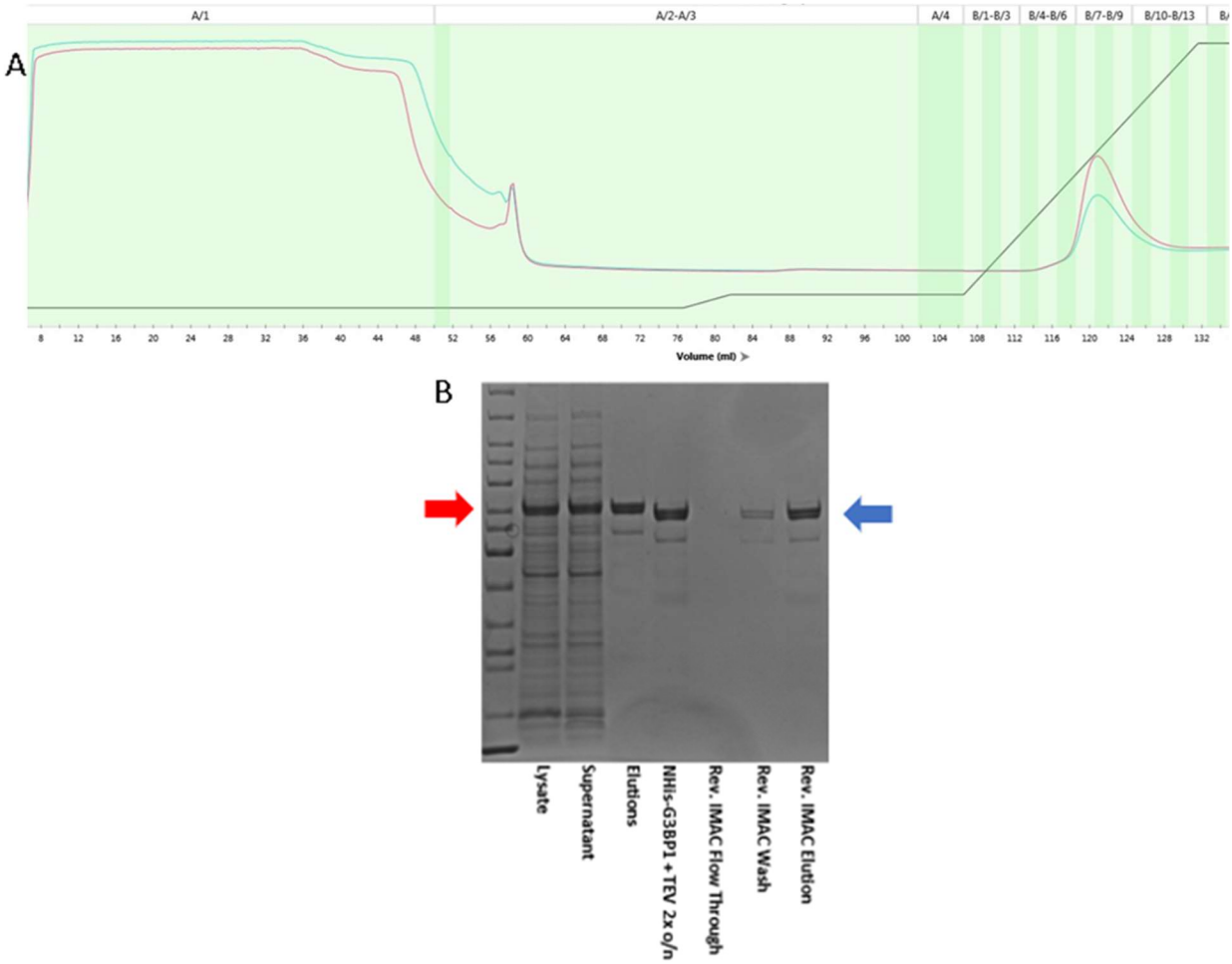

Figure 20: IMAC purification of NHis-G3BP1 and reverse IMAC purification of G3BP1 – A is the chromatogram of the IMAC purification of NHis-G3BP1 where the black line is the imidazole gradient, the red line is the A_{280} trace and the blue line is the A_{260} trace monitoring the protein and nucleic acid presence in the solution leaving the FPLC from the Ni^{2+}-NTA column. B is the SDS-PAGE gel monitoring the molecular weight of NHis-G3BP1 during the lysis and IMAC purification steps and the reverse IMAC collections of G3BP1 after TEV cleavage. The red arrow is pointing at the band corresponding to NHis-G3BP1 (70 kDa).

and the blue line is pointing at the band corresponding to G3BP1 after the his tag is removed (67 kDa) indicating a shift that is brought about by the TEV reaction.4

4.7.2 TEV Cleavage of Elution Fractions

After the 15 mL IMAC elution sample was taken from dialysis the protein solution measured 34.2 μM. TEV was added to the dialysis tubing (2% (mole/mole)), and fresh dialysis buffer was made, supplemented with 0.5 mM EDTA to enhance the TEV activity and kept at 4 ℃ for 48 hours.

4.7.3 Reverse IMAC of TEV and NHis-G3BP1

The dialysis sample was removed and absorbance measurements at 260, 280, 350 and 600 nm were checked. The protein increased at all wavelengths which indicates the presence of aggregate particles in the solution. Reverse IMAC purification was performed to separate the protein from TEV and its affinity tag. A buffer of 20 mM HEPES with 1 mM DTT (pH 7.5) was equilibrated over the column and in the wash step and supplemented with 500 mM imidazole in the elution step. After measuring the A_{280} of the fractions with UV-vis, the protein was found primarily in the elution collection. Wash buffer was made with no imidazole so that there would be less competitive displacement from the IMAC resin by the presence of imidazole. However, it is possible that the protein was charged enough to stick to the column and needs a small amount of imidazole (~20 mM) to be captured in the wash fractions without releasing the his-tag of the protein or TEV. All fractions were examined with SDS-PAGE, and each appeared with a shift in molecular weight equal to the loss of the his-tag, so they were combined as one sample (Figure 20B). The reverse IMAC equilibration buffer was made without salt in preparation for the ensuing AEX the next day and the sample was placed into a fresh solution of 20 mM HEPES, 1 mM DTT (pH 7.5) at 4 ℃ overnight.

4.7.4 AEX of G3BP1

AEX was performed on the cleaved sample to remove contaminants from the protein solution. After the sample was taken from the dialysis tubing, it was prepared for AEX by filtering through a 0.22 μm syringe filter to prevent any aggregates from clogging the column. Next, the absorbance was measured at 260, 280, 350 and 600 nm to evaluate the nucleic acid, protein, and insoluble particle content of the sample solution before running AEX, and the absorbance measurements indicated none of these species were present. Filtering the protein removes the insoluble species from the sample filtrate meaning the protein solution must have precipitated entirely during the dialysis step prior to AEX. After multiple failed attempts to prepare the protein in conditions of low salt, it was determined that the protein is not suitable for AEX due to its propensity to aggregate under conditions of low salt. As a result, future purifications would be stopped after the reverse IMAC step, and buffer conditions would be limited to higher sodium chloride concentrations. As with previous attempts, a completely new purification of a G3BP1-expressed cell pellet was required.

4.8 Pellet #4 of Expression #3

After it was determined that low salt was the variable responsible for protein instability *in vitro*, a new pellet was lysed, and its protein purified according to sections 3.1.6–3.1.8. All purifications and cleavage steps were then performed with a minimum of 250 mM sodium chloride since previous steps performed at this concentration were able to maintain protein solubility in solution. Since SDS-PAGE gels revealed a small number of contaminants, if any, following TEV cleavage and reverse IMAC purification, this would mark the final affinity chromatography technique for future purifications of G3BP1. Since AEX requires concentrations of sodium chloride in minimal amounts, this purification step would be skipped in future purifications.

4.8.1 IMAC Purification of pET11a-BL21(DE3)-NHis-G3BP1

A new, 3 g pellet was lysed and purified on the FPLC with 0.1 mM PMSF and NHis-G3BP1 IMAC equilibration buffer according to section 3.1.6. There was an obvious A_{280} peak in the chromatogram during the elution step and the SDS-PAGE gel showed a band corresponding to NHis-G3BP1 (Figure 21). The elution fractions were pooled, placed in dialysis tubing in fresh equilibration buffer and left at 4 ℃ overnight to remove the imidazole from the protein solution.

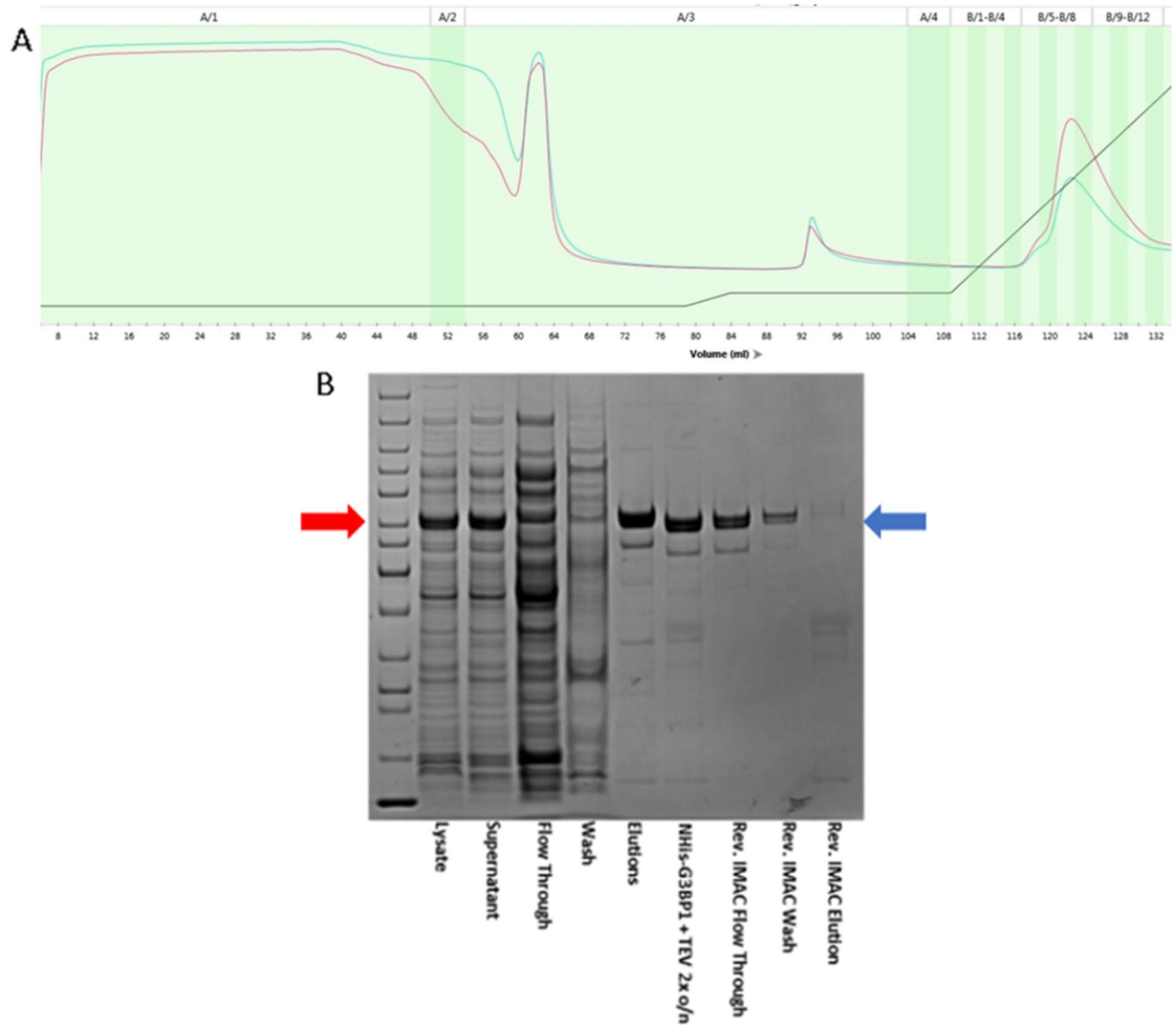

Figure 21:5 : IMAC purification of NHis-G3BP1 and reverse IMAC purification of G3BP1 – A is the chromatogram of the IMAC purification of NHis-G3BP1 where the black line is the imidazole gradient, the red line is the A_{280} trace and the blue line is the A_{260} trace monitoring the protein and nucleic acid presence in the solution leaving the FPLC from the Ni^{2+}-NTA column. B is the SDS-PAGE gel monitoring the molecular weight of NHis-G3BP1 during the lysis and IMAC purification steps and the reverse IMAC collections of G3BP1 after TEV cleavage. The red arrow is pointing at the band corresponding to NHis-G3BP1

(70 kDa) and the blue line is pointing at the band corresponding to G3BP1 after the his tag is removed (67 kDa) indicating a shift that is brought about by the TEV reaction.6

4.8.2 TEV Cleavage of Elution Fractions

20 mL of protein solution was retrieved from the dialysis tubing, and using the A_{280} measurement, the concentration was determined to be 66.3 μM. Next, 2% TEV (mole/mole) was added to the dialysis tubing to cleave the his-tag. This was placed into fresh equilibration buffer at 4 ℃ for 48 hours of dialysis to remove even more imidazole from solution and allow the TEV reaction to occur.

4.8.3 Reverse IMAC of TEV and NHis-G3BP1

The dialyzed sample was removed, and the absorbance measurements were taken to compare against the flow through, wash and elution fractions that were collected from the reverse IMAC purification. Minimal light scattering was observed which was interpreted as successful buffer conditions for protein stability during the 3 days since purification. The Ni^{2+}-NTA resin was equilibrated with dialysis buffer and the sample was allowed to flow through the column. The wash step was performed with IMAC equilibration buffer supplemented with 20 mM imidazole to displace protein that was bound through interactions less prevalent than the his-tag. The elution of the remaining species bound to the column was achieved with 500 mM imidazole supplemented in the equilibration buffer. Aliquots of each collected step were taken to examine the efficiency of the TEV cleavage using SDS-PAGE (Figure 21B). The gels and absorbance measurements indicated that most of the protein was found in the flow through and wash fractions. Additionally, there seemed to be minimal contaminants visualized by the gels which made the additional step of AEX unnecessary. The results were considered a success regarding the appropriate methods that should be replicated for future purifications and TEV

cleavages and are detailed in sections 3.1.6–3.1.8. These purified samples were then used in condition tests and SEC analysis described in the next sections.

5 Sample Tests for NMR-Compliant Conditions

Salt concentration, pH, and sample concentration were tested on the purified G3BP1 protein in solution for the optimal conditions to run NMR experiments described in section 1.2.6. Using the cleaved protein collected from the reverse IMAC purification in the previous section, samples were monitored in lower salt concentrations and pH values near the isoelectric point of G3BP1 (both above and below), and concentrations near 20 μM and over 100 μM. The viability of the protein solutions was assessed with UV-vis measurements to evaluate the amount of nucleic acid, protein, and light-scattering particles in each sample at each condition. Additionally, SDS-PAGE gels were used to monitor the relative amount and identity of the species in the protein solution as they changed in the buffer conditions.

5.1 G3BP1 Sample Tests in Buffers Above the Isoelectric Point

Tests were conducted at pH 6.0, 6.5, and 7.5 in which the samples were spin-concentrated to 120 μM and dialyzed over three days in dialysis tubing and these were compared to the sample that was collected in section 4.8.3. Three conditions were tested, 50 mM MES with 200 mM sodium chloride buffer at pH 6.0 and 6.5, along with 50 mM HEPES containing 200 mM sodium chloride buffer at pH 7.5. Afterward, the samples were analyzed by their absorbances at 260, 280, 350 and 600 nm and SDS-PAGE to monitor stability (Figures 22A and 22B). Regarding light-scattering, the sample performed as well at pH 6.0 as it did at pH 6.5 in MES buffer, and although HEPES was the buffer during all prior purification steps, it produced the most aggregation at the higher sample/lower salt concentrations. To maintain uniformity between treatment of the testing species, all samples were spun at 20,000 x*g* for 20 minutes to

pellet any aggregates, however, the light scattering at 350 and 600 nm increased dramatically in all three samples as a result and the degradation of the protein was noticeable in the SDS-PAGE gels (Figures 22A and 22B). The effect of the spinning was not able to be tested for its effect on aggregation via UV-vis-measured light scattering since the control was also spun and not compared to the control before spinning. However, the scattering effect was not observed in the control sample that was maintained in equilibration buffer from the reverse IMAC purification. The control sample differed from the conditions tested by a greater concentration of sodium chloride by 50 mM. Again, salt was implicated as a factor in protein stability, although the SDS-PAGE gels indicated that protein degradation was occurring in the control sample as well even though it was not measurable with UV-vis.

A

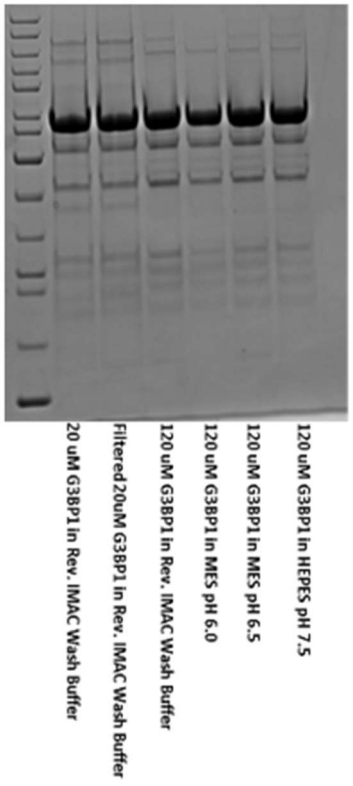

B

	Rev. IMAC Collection	MES pH 6.0	MES pH 6.5	HEPES pH 7.5
Abs_{260}	1.350/1.348	1.026/2.790	1.215/1.278	1.439/1.445
Abs_{280}	2.157/2.155	1.639/2.820	1.969/1.997	2.080/2.098
Abs_{350}	0.018/0.031	0.002/0.965	0.007/0.031	0.331/0.331
Abs_{600}	0.000/0.017	0.000/0.311	0.000/0.000	0.311/0.311

C

	Rev. IMAC Collection	MES pH 6.5 200 mM NaCl	MES pH 6.5 100 mM NaCl	PIPPS pH 4.5 200 mM NaCl	PIPPS pH 4.5 100 mM NaCl
Abs_{260}	0.351	0.130	0.310	0.079	0.034
Abs_{280}	0.497	0.127	0.240	0.031	0.027
Abs_{350}	0.012	0.003	0.065	0.000	0.003
Abs_{600}	0.000	0.000	0.000	0.000	0.000

Figure 22: Stability tests of G3BP1 in different buffer conditions – A is the SDS-PAGE gel of G3BP1 before and after dialyzing in different buffer conditions to test for the change in the relative abundance of species in the protein solution. There appears to be no difference between each of the buffer conditions with respect to the presence of the bands. B shows the UV-vis

measurements at the wavelengths of 260, 280, 350 and 600 nm to account for the amounts of nucleic acids, protein, and light-scattering particles, respectively. The first number in each cell corresponds to the value before spinning and the second value (separated by the hyphen) correspond to the values after spinning at 20000 xg for 20 minutes. C shows the UV-vis measurements of the protein solution before and after dialyzing in the respective buffers where the pH, buffer system and sodium chloride conditions varied.

5.2 G3BP1 Sample Tests in Buffers Below the Isoelectric Point

Since the protein was lost to aggregation or degradation at pH values above the isoelectric point of the protein (pH 5.71), similar tests were run below this value in pH 4.5, 30 mM PIPPS buffer, where 30 mM PIPPS is the concentration limit of solubility. In addition to the pH and buffer system changes, salt tests were conducted at 100 and 200 mM sodium chloride. Additionally, 50 mM MES (pH 6.5) buffer was tested at 100 and 200 mM sodium chloride alongside PIPPS and the original reverse IMAC sample elution from 4.8.3. These samples were buffer exchanged through desalting columns before spin-concentrating afterward. The absorbance readings in Figure 22C suggest most protein was lost to aggregation in both samples of PIPPS as the A_{280} measurements were near zero, and light scattering was present in the sample buffered with MES and 200 mM sodium chloride. Due to the low concentrations of remaining protein, the samples were spin-concentrated to prepare gels that would relay information about the state of the samples. Unfortunately, the spinning led to a complete loss of protein within the PIPPS, and MES samples according to the UV-vis measurements and the gels were revealed no bands. More condition tests are underway to discover a buffer system that is amenable to both NMR experiments and stable G3BP1 as described in section 1.2.6.

6 SEC Analysis

Size exclusion was run on the ENrich SEC 650 10 x 300 column with G3BP1 taken from the reverse IMAC wash collection in section 4.8.3. It was performed to separate species at 55 and 70 kDa that are observed in the gels after each purification step and to measure the

quaternary structure of the protein in solution that is not possible in SDS-PAGE denaturing conditions.

6.1 SEC Purification of G3BP1 in Solution

The G3BP1 sample from section 4.8.3 was spin-concentrated to 350 µL of 66.4 µM protein. The SEC column was equilibrated with IMAC equilibration buffer before loading the sample through the 350 µL loop connected to the SEC 650 column of the FPLC. The elution was monitored by the change in absorbance at 280 nm with respect to the run volume using the attached UV-vis. The sample was collected in intervals of 0.5 mL to capture a singular species in each fraction and SDS-PAGE was used to identify their presence (Figure 23). However, the resolution of the column did not allow enough volume between species and the accompanying spectrum had peaks with no separation leading to SDS-PAGE gel bands at 55 and 68 kDa in all collections. To address this limitation, future SEC experiments will be run on columns with larger resin volumes that facilitate better resolution for separating species with more volume between those of comparable size.

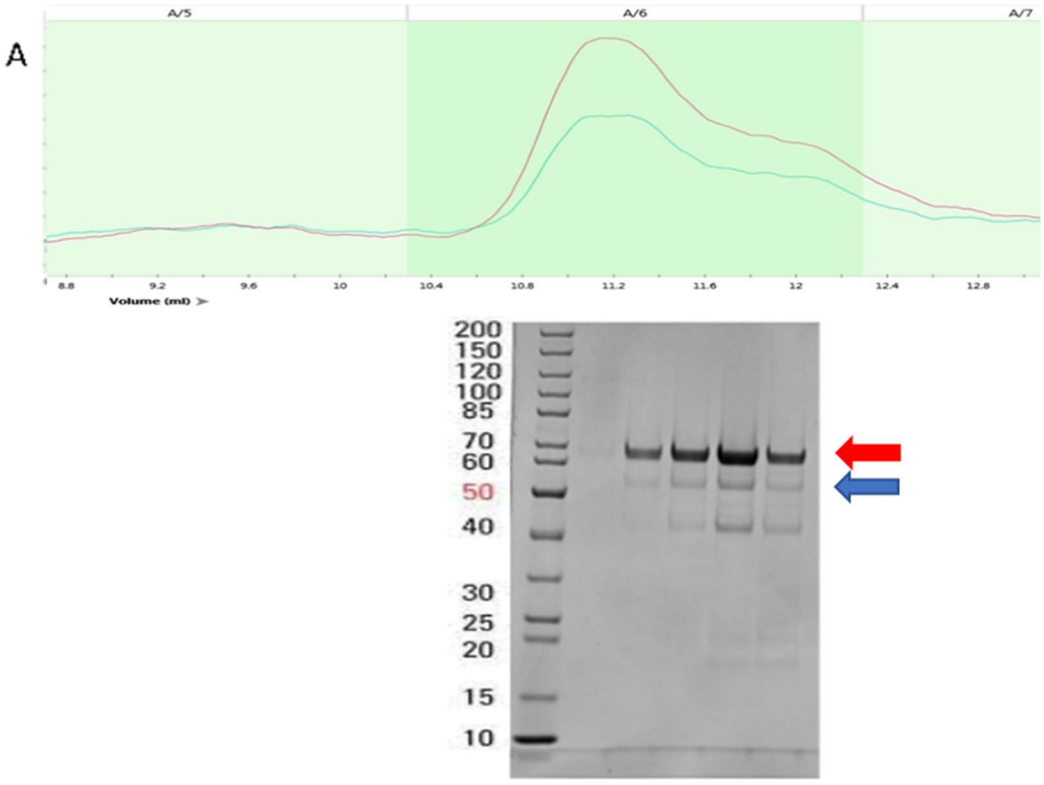

Figure 23:7 SEC purification and analysis of G3BP1 – A is the chromatogram of G3BP1 from the SEC run focusing on the elution peak where the red and green line are the A_{260} and A_{280} traces, respectively, to monitor the nucleic acid and protein elution volumes. The elution volume is 11.4 mL and was fit to the equation Mass (kDa) = $501486.3*e^{(-.65x)} + -2.1$ from the protein standards' calibration curve. This equation produces the mass of G3BP1 in solution which is 5.95 times larger than the known mass of G3BP1 which indicates quaternary structure of a hexamer. B is the accompanying SDS-PAGE gel of the collected elution fractions in 0.5 mL increments in an attempt to separate the 70 kDa species (red arrow) from the 55 kDa species (blue arrow) which was unsuccessful.

6.2 SEC Analysis of G3BP1 Quaternary Composition in Solution

Because SDS-PAGE gels are run in a denatured environment, it is not possible to determine quaternary structure among proteins *in vitro.* Therefore, SEC was used to determine the mass of the protein in a more natural buffer system. Calculating the G3BP1 molecular mass from the SEC data is possible given the protein standards that were run on the column previously to identify the relationship between molecular weight and retention volume. The standards produced a calibration curve with a logarithmic relationship, and the data were fit to the equation Mass (kDa) = $501486.3 \cdot e^{(-0.65x)} - 2.1$. During the SEC experiment there was a spike of absorbance at 280 nm in the spectrum at 11.4 mL that was collected and verified by SDS-PAGE

as G3BP1 (Figure 23). According to the calibration curve equation, 11.4 mL corresponds to a molecular weight of 310.2 kDa which is 5.95 times the weight of the monomer. Although a hexamer is a possible quaternary structure of G3BP1, there exist issues with the validity of the SEC. For instance, globular proteins were used as standards to produce the calibration curve which have a compact size and smaller effective radii compared to non-globular proteins. This makes it difficult to use in comparison to G3BP1 which contains multiple intrinsically disordered regions that increase the observed size and, by effect, molecular mass. Native-PAGE gels will be attempted in upcoming tests for their ability to observe the weight of the oligomers that might exist *in vitro* and validate the binding partners of the protein under non-denaturing conditions that were suggested by the SEC results.

7 TEV Production for His-Cleavage Reactions

TEV was produced for cleavage reactions to remove the his-tag from NHis-G3BP1 to enable biochemical studies of the G3BP1 protein without non-native amino acids that would alter results of studies intended to describe the structure and interactions of Human G3BP1 protein. To make enough TEV for multiple cleavage reactions, BL21(DE3) *E. coli* cells were grown and IPTG was used to induce expression of the enzyme as described in section 3.2.1. SDS-PAGE was used to monitor the growth of TEV throughout the process. Afterward, the protein was lysed from the cells and purified by IMAC purification where the FPLC chromatogram and SDS-PAGE were used to analyze the presence and purity of TEV which was described in section 3.2.2. Finally, UV-vis measurements were taken to quantify the amount of TEV produced for future cleavage reactions of the his-tags of genetically engineered proteins.

7.1 TEV Growth and Expression

The growth and expression of TEV was performed according to the protocol established by the Murray lab. Specifically, timepoints of the process were sampled, normalized to their respective A_{600} for comparison of TEV presence in the expression system, and examined through SDS-PAGE (Figure 24B). The TEV was grown in two 1 L cultures that were harvested separately and weighed 8.3 and 8.8 g, respectively, before freezing in liquid nitrogen and storing at -80°C for future use. During the growth and expression, the thickest bands were observed near 48 kDa, although the predicted mass is 27 kDa. This indicates the presence of species other than TEV, although the TEV cleavage reactions that were administered with NHis-G3BP1 were not affected by their presence and they were removed during the purification process shown in Figure 24C.

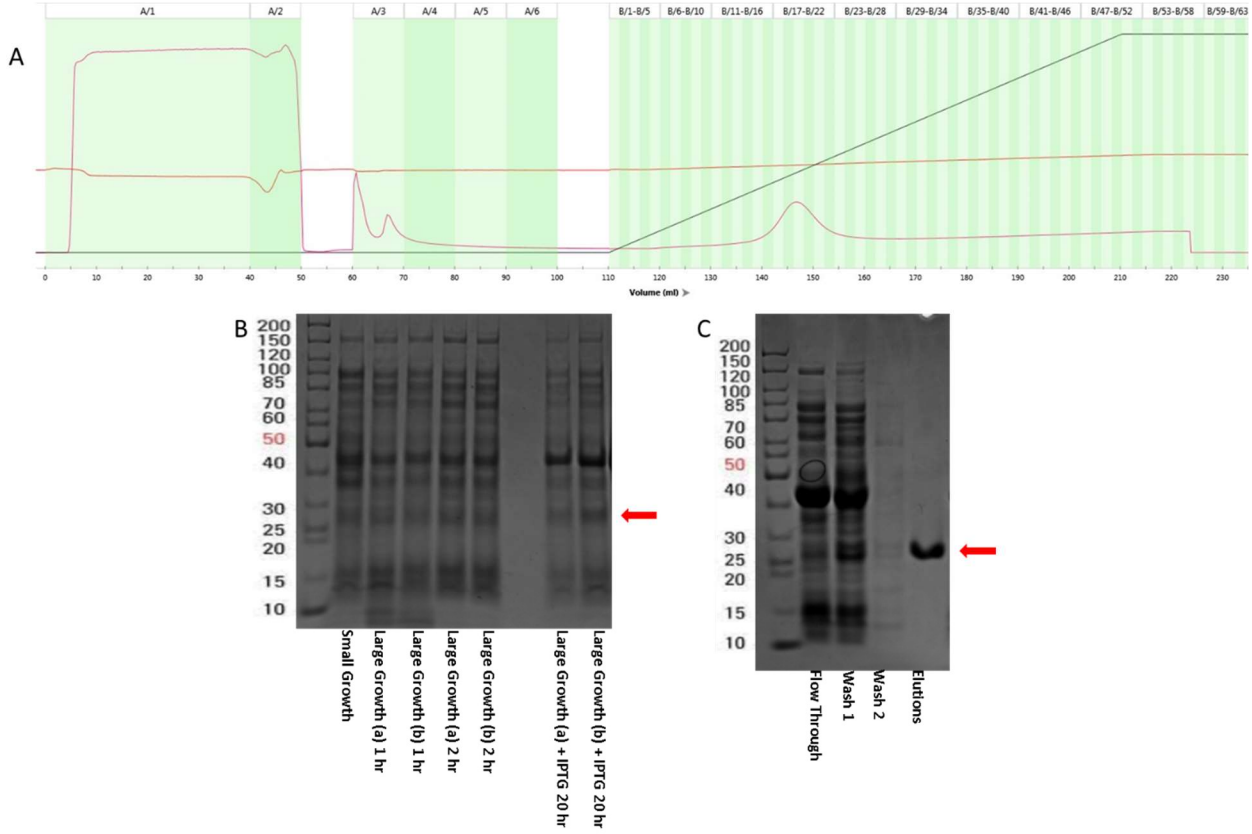

Figure 24: TEV growth, expression, and purification – A is the chromatogram of the IMAC purification of TEV where the black line is the gradient of imidazole, and the red line is the A_{280} trace monitoring the volume at which the protein eluted from the

FPLC column. B is the growth and expression of TEV where the red arrow is pointing at the bands corresponding to TEV's weight. The band becomes somewhat darker after IPTG is added to the cultures. C is the SDS-PAGE gel of the purification fractions from the IMAC where the red arrow is pointing at the location where TEV is found. In the elution fraction, there appears to be only one species at the molecular weight of TEV suggesting successful isolation of the enzyme.**Error! Bookmark not defined.**

7.2 TEV IMAC Purification

An 8.3 g pellet of TEV was lysed and purified over a Ni^{2+}-NTA IMAC column on the FPLC according to section 3.2.2 to produce pure TEV protease for future cleavage reactions with NHis-G3BP1 to remove the affinity tag attached to the protein. The chromatogram in Figure 24A shows a peak during the elution step that was expected to be the TEV protein since it has an affinity his-tag and should be isolated from the lysate by binding to the Ni^{2+}-NTA IMAC column. The flow through, wash and elution fractions were collected separately and analyzed with SDS-PAGE which indicated the elution fractions contained the TEV enzyme according to its predicted molecular weight (27 kDa) and were free from contaminants (Figure 24C). The total yield was 10 mL of 37.6 μM TEV which was diluted twofold into its final storage conditions described in section 3.2.2 and stored at −80℃ for use in future his-tag cleavage reactions of G3BP1.

8 ^{15}N – Labelled pET11a-BL21(DE3)-NHis-G3BP1

NMR related studies are possible when the protein that is being studied is composed of magnetic nuclei such as ^{15}N. Expressing the protein in cells that are exposed to media that has every nitrogen source converted to ^{15}N gives the cell no other chance of producing the protein with any non-labelled nitrogen during expression. This makes 2D-NMR studies more effective when the species are enriched with magnetic nuclei. By analyzing the production of NHis-G3BP1 with SDS-PAGE before and after induction, it was possible to verify the presence of the protein when the media was switched to nitrogen sources containing only ^{15}N.

8.1 ^{15}N – Labelled Growth and Expression of pET11a-BL21(DE3)-NHis-G3BP1

Enriched, ^{15}N-pET11a-NHis-G3BP1 was expressed in BL21(DE3) cells as reported in section 3.1.5. After 3 hours of expression, the cells were pelleted and weighed 1.8 g before freezing at −80 °C. SDS-PAGE samples were taken of the small culture, two large cultures, suspended pellets of the two large cultures in M9 media without IPTG, and then hourly after IPTG (Figure 25). The results show minimal NHis-G3BP1 present before induction and a steady accumulation of the corresponding band throughout the expression timeline. It is not possible to calculate the effectiveness of the amino acid labeling without further studies. These will be implemented in future work by analyzing MALDI – TOF data of the purified sample for the relative abundances of the molecular weights corresponding to labeled and unlabeled protein. After determining the fraction of labelled protein, isolating it from the cell lysate, and cleaving the his-tags, 2-D NMR experiments such as HSQC are possible for structural studies of G3BP1.

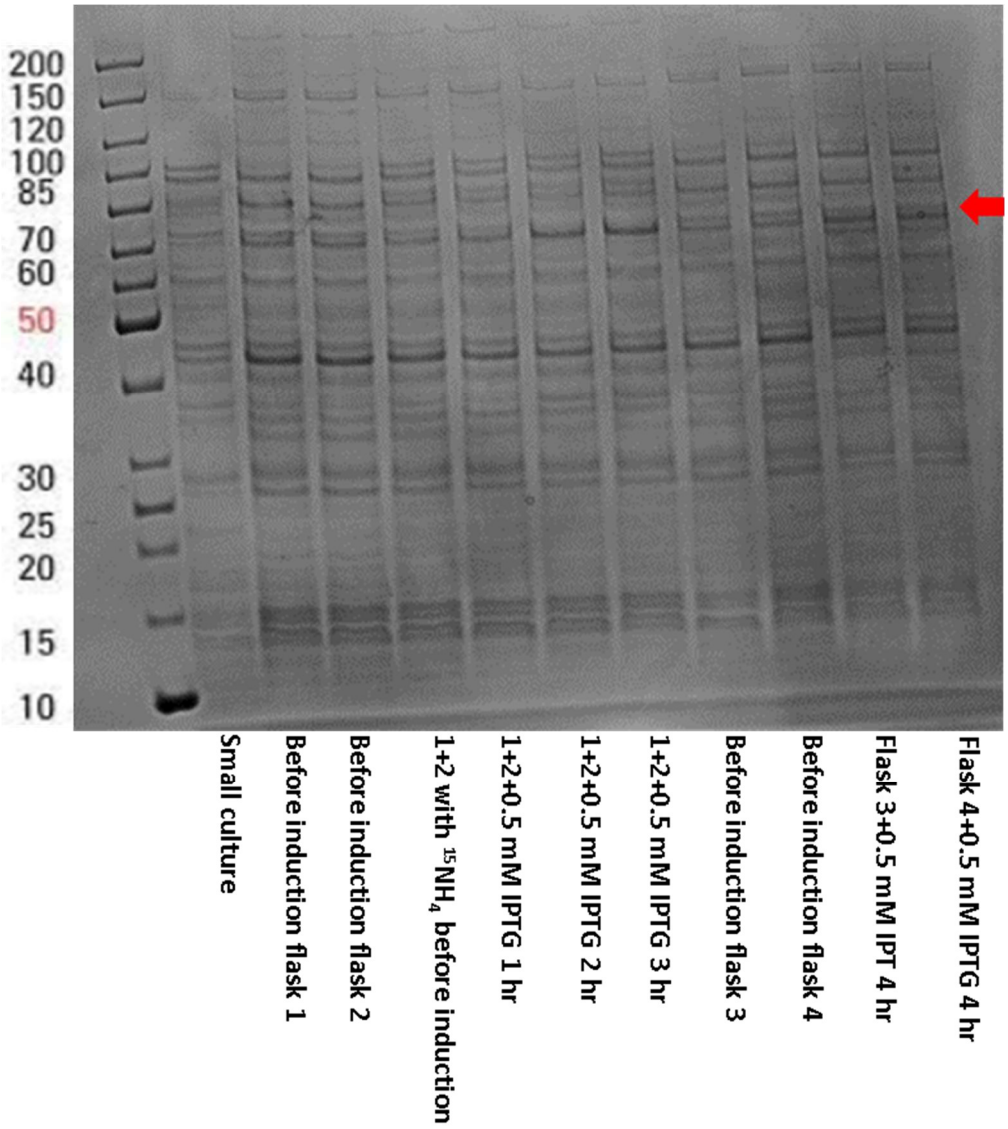

Figure 25: ^{15}N-labelled growth and unlabeled growth of pET11a-NHis-G3BP1 with samples taken of timepoints during the growth and expression. The red arrow is pointing at the bands corresponding to NHis-G3BP1 at its observed molecular weight (70 kDa) during these processes. Flasks 1 – 4 originate from the small culture before it was split into 4 separate large culture growths of 1 L each. Flasks 3 and 4 were expressed in unlabeled media and Flasks 1 and 2 were combined (1+2) and pelleted before resuspension and induction in labelled media. Before IPTG there should be no NHis-G3BP1 present, and its corresponding band should get progressively darker during the expression time. There appears to be some NHis-G3BP1 in each flask before IPTG is added, but it is noticeably less than at the end of the expression time.

9 Conclusion

The NHis-G3BP1 protein was successfully designed and extracted from the *E. coli* expression system where the affinity tag was removed by the TEV protease that was produced in-house. IMAC, AEX and SEC purification techniques were applied on the extracted protein

solution. The affinity his-tag allowed G3BP1 to be collected from a single cell lysate in amounts up to 165 mg; however, the low-salt conditions necessary for AEX proved to be not suitable for maintaining soluble G3BP1 and ultimately, the technique was discontinued after this was determined. SEC was not successful in separating the remaining species observed in the SDS-PAGE gel at 68 and 55 kDa after IMAC and reverse IMAC steps, but the peak elution time observed in the SEC chromatogram revealed that the protein exists as a hexamer in solution. The validity of this result is questionable as the intrinsically disordered regions of the G3BP1 protein structure can deviate from the mass expectancy derived by the globular protein standards' calibration curve.

The protein solution was tested at NMR-relevant conditions such as high protein concentrations, lower pHs and lower sodium chloride concentrations which resulted in aggregation and loss of protein that was verified by SDS-PAGE and UV-vis analysis. Ultimately, these shortcomings need to be addressed for future solution state NMR experiments to gain information about the structure of the G3BP1 species. After rectifying this dilemma, the NMR experiments can be used to observe changes in the structure after biologically relevant species are introduced to the solution to uncover the specific interactions between G3BP1 and other proteins and potential post-translational modifications.

References

(1) Patel, A.; Lee, H. O.; Jawerth, L.; Maharana, S.; Jahnel, M.; Hein, M. Y.; Stoynov, S.; Mahamid, J.; Saha, S.; Franzmann, T. M.; Pozniakovski, A.; Poser, I.; Maghelli, N.; Royer, L. A.; Weigert, M.; Myers, E. W.; Grill, S.; Drechsel, D.; Hyman, A. A.; Alberti, S. A Liquid-to-Solid Phase Transition of the ALS Protein FUS Accelerated by Disease Mutation. *Cell* **2015**, *162* (5), 1066–1077. https://doi.org/10.1016/J.CELL.2015.07.047.

(2) Tompa, P.; Csermely, P. The Role of Structural Disorder in the Function of RNA and Protein Chaperones. *FASEB J.* **2004**, *18* (11), 1169–1175. https://doi.org/10.1096/FJ.04-1584REV.

(3) Ivanyi-Nagy, R.; Davidovic, L.; Khandjian, E. W.; Darlix, J. L. Disordered RNA Chaperone Proteins: From Functions to Disease. *Cell. Mol. Life Sci.* **2005**, *62* (13), 1409–1417. https://doi.org/10.1007/S00018-005-5100-9.

(4) Gebauer, F.; Schwarzl, T.; Valcárcel, J.; Hentze, M. W. RNA-Binding Proteins in Human Genetic Disease. *Nat. Rev. Genet. 2020 223* **2020**, *22* (3), 185–198. https://doi.org/10.1038/s41576-020-00302-y.

(5) Van Der Lee, R.; Buljan, M.; Lang, B.; Weatheritt, R. J.; Daughdrill, G. W.; Dunker, A. K.; Fuxreiter, M.; Gough, J.; Gsponer, J.; Jones, D. T.; Kim, P. M.; Kriwacki, R. W.; Oldfield, C. J.; Pappu, R. V.; Tompa, P.; Uversky, V. N.; Wright, P. E.; Babu, M. M. Classification of Intrinsically Disordered Regions and Proteins. *Chem. Rev.* **2014**, *114* (13), 6589–6631. https://doi.org/10.1021/CR400525M/ASSET/IMAGES/LARGE/CR-2013-00525M_0006.JPEG.

(6) Turner, M.; DÍaz-Muñoz, M. D. RNA-Binding Proteins Control Gene Expression and Cell Fate in the Immune System. *Nat. Immunol. 2017 192* **2018**, *19* (2), 120–129. https://doi.org/10.1038/s41590-017-0028-4.

(7) Banani, S. F.; Lee, H. O.; Hyman, A. A.; Rosen, M. K. Biomolecular Condensates: Organizers of Cellular Biochemistry. *Nat. Rev. Mol. Cell Biol.* **2017**, *18* (5), 285–298. https://doi.org/10.1038/NRM.2017.7.

(8) Hentze, M. W.; Castello, A.; Schwarzl, T.; Preiss, T. A Brave New World of RNA-Binding Proteins. *Nat. Rev. Mol. Cell Biol. 2018 195* **2018**, *19* (5), 327–341. https://doi.org/10.1038/nrm.2017.130.

(9) Brangwynne, C. P.; Eckmann, C. R.; Courson, D. S.; Rybarska, A.; Hoege, C.; Gharakhani, J.; Jülicher, F.; Hyman, A. A. Germline P Granules Are Liquid Droplets That Localize by Controlled Dissolution/Condensation. *Science (80-.).* **2009**, *324* (5935), 1729–1732. https://doi.org/10.1126/SCIENCE.1172046/SUPPL_FILE/BRANGWYNNE.SOM.PDF.

(10) Brangwynne, C. P.; Mitchison, T. J.; Hyman, A. A. Active Liquid-like Behavior of Nucleoli Determines Their Size and Shape in Xenopus Laevis Oocytes. *Proc. Natl. Acad. Sci. U. S. A.* **2011**, *108* (11), 4334–4339. https://doi.org/10.1073/PNAS.1017150108/ASSET/9530B829-7948-4296-BE4C-95F7DA1ED7C4/ASSETS/GRAPHIC/PNAS.1017150108EQ3.GIF.

(11) Alberti, S.; Gladfelter, A.; Mittag, T. Considerations and Challenges in Studying Liquid-Liquid Phase Separation and Biomolecular Condensates. *Cell* **2019**, *176* (3), 419. https://doi.org/10.1016/J.CELL.2018.12.035.

(12) Lodge, T. P.; Muthukumar, M. Physical Chemistry of Polymers: Entropy, Interactions, and Dynamics. **1996**.

(13) F, P.; F, M.; I, D.; M, D.; D, F.; L, D.; A, D.; F, S.; B, T. A Ras-GTPase-Activating Protein SH3-Domain-Binding Protein. *Mol. Cell. Biol.* **1996**, *16* (6), 2561–2569.

https://doi.org/10.1128/MCB.16.6.2561.

(14) Gallouzi, I.; Parker, F.; Chebli, K.; Maurier, F.; Labourier, E.; Barlat, I.; Capony, J.-P.; Tocque, B.; Tazi, J. A Novel Phosphorylation-Dependent RNase Activity of GAP-SH3 Binding Protein: A Potential Link between Signal Transduction and RNA Stability. *Mol. Cell. Biol.* **1998**, *18* (7), 3956. https://doi.org/10.1128/MCB.18.7.3956.

(15) Harmon, T. S.; Holehouse, A. S.; Rosen, M. K.; Pappu, R. V. Intrinsically Disordered Linkers Determine the Interplay between Phase Separation and Gelation in Multivalent Proteins. *Elife* **2017**, *6*. https://doi.org/10.7554/ELIFE.30294.

(16) Tourrière, H.; Chebli, K.; Zekri, L.; Courselaud, B.; Blanchard, J. M.; Bertrand, E.; Tazi, J. The RasGAP-Associated Endoribonuclease G3BP Assembles Stress Granules. *J. Cell Biol.* **2003**, *160* (6), 823–831. https://doi.org/10.1083/JCB.200212128.

(17) Guillén-Boixet, J.; Kopach, A.; Holehouse, A. S.; Wittmann, S.; Jahnel, M.; Schlüßler, R.; Kim, K.; Trussina, I. R. E. A.; Wang, J.; Mateju, D.; Poser, I.; Maharana, S.; Ruer-Gruß, M.; Richter, D.; Zhang, X.; Chang, Y. T.; Guck, J.; Honigmann, A.; Mahamid, J.; Hyman, A. A.; Pappu, R. V.; Alberti, S.; Franzmann, T. M. RNA-Induced Conformational Switching and Clustering of G3BP Drive Stress Granule Assembly by Condensation. *Cell* **2020**, *181* (2), 346. https://doi.org/10.1016/J.CELL.2020.03.049.

(18) Vognsen, T.; Møller, I. R.; Kristensen, O. Crystal Structures of the Human G3BP1 NTF2-Like Domain Visualize FxFG Nup Repeat Specificity. *PLoS One* **2013**, *8* (12). https://doi.org/10.1371/JOURNAL.PONE.0080947.

(19) Varadi, M.; Anyango, S.; Deshpande, M.; Nair, S.; Natassia, C.; Yordanova, G.; Yuan, D.; Stroe, O.; Wood, G.; Laydon, A.; Zídek, A.; Green, T.; Tunyasuvunakool, K.; Petersen, S.; Jumper, J.; Clancy, E.; Green, R.; Vora, A.; Lutfi, M.; Figurnov, M.; Cowie, A.; Hobbs, N.; Kohli, P.; Kleywegt, G.; Birney, E.; Hassabis, D.; Velankar, S. AlphaFold Protein Structure Database: Massively Expanding the Structural Coverage of Protein-Sequence Space with High-Accuracy Models. *Nucleic Acids Res.* **2022**, *50* (D1), D439–D444. https://doi.org/10.1093/NAR/GKAB1061.

(20) Jumper, J.; Evans, R.; Pritzel, A.; Green, T.; Figurnov, M.; Ronneberger, O.; Tunyasuvunakool, K.; Bates, R.; Žídek, A.; Potapenko, A.; Bridgland, A.; Meyer, C.; Kohl, S. A. A.; Ballard, A. J.; Cowie, A.; Romera-Paredes, B.; Nikolov, S.; Jain, R.; Adler, J.; Back, T.; Petersen, S.; Reiman, D.; Clancy, E.; Zielinski, M.; Steinegger, M.; Pacholska, M.; Berghammer, T.; Bodenstein, S.; Silver, D.; Vinyals, O.; Senior, A. W.; Kavukcuoglu, K.; Kohli, P.; Hassabis, D. Highly Accurate Protein Structure Prediction with AlphaFold. *Nat. 2021 5967873* **2021**, *596* (7873), 583–589. https://doi.org/10.1038/s41586-021-03819-2.

(21) Yang, P.; Mathieu, C.; Kolaitis, R. M.; Zhang, P.; Messing, J.; Yurtsever, U.; Yang, Z.; Wu, J.; Li, Y.; Pan, Q.; Yu, J.; Martin, E. W.; Mittag, T.; Kim, H. J.; Taylor, J. P. G3BP1 Is a Tunable Switch That Triggers Phase Separation to Assemble Stress Granules. *Cell* **2020**, *181* (2), 325-345.e28. https://doi.org/10.1016/J.CELL.2020.03.046.

(22) Nallamsetty, S.; Kapust, R. B.; Tözsér, J.; Cherry, S.; Tropea, J. E.; Copeland, T. D.; Waugh, D. S. Efficient Site-Specific Processing of Fusion Proteins by Tobacco Vein Mottling Virus Protease in Vivo and in Vitro. *Protein Expr. Purif.* **2004**, *38* (1), 108–115. https://doi.org/10.1016/J.PEP.2004.08.016.

(23) Nam, H.; Hwang, B. J.; Choi, D. Y.; Shin, S.; Choi, M. Tobacco Etch Virus (TEV) Protease with Multiple Mutations to Improve Solubility and Reduce Self-Cleavage Exhibits Enhanced

Enzymatic Activity. *FEBS Open Bio* **2020**, *10* (4), 619–626. https://doi.org/10.1002/2211-5463.12828.

(24) Kelly, A. E.; Ou, H. D.; Withers, R.; Dötsch, V. Low-Conductivity Buffers for High-Sensitivity NMR Measurements. *J. Am. Chem. Soc.* **2002**, *124* (40), 12013–12019. https://doi.org/10.1021/JA026121B/ASSET/IMAGES/MEDIUM/JA026121BN00001.GIF.

(25) Cooper, R. A.; Lichter, R. L.; Roberts, J. D. PH-Dependent Nuclear Magnetic Resonance Spectra of N-Enriched Glycine. Line Shape and Relaxation Studies. *J. Am. Chem. Soc.* **1973**, *95* (11), 3724–3729. https://doi.org/10.1021/JA00792A042/ASSET/JA00792A042.FP.PNG_V03.

(26) Chhabra, S.; Fischer, P.; Takeuchi, K.; Dubey, A.; Ziarek, J. J.; Boeszoermenyi, A.; Mathieu, D.; Bermel, W.; Davey, N. E.; Wagner, G.; Arthanari, H. 15N Detection Harnesses the Slow Relaxation Property of Nitrogen: Delivering Enhanced Resolution for Intrinsically Disordered Proteins. *Proc. Natl. Acad. Sci. U. S. A.* **2018**, *115* (8), E1710–E1719. https://doi.org/10.1073/PNAS.1717560115/SUPPL_FILE/PNAS.1717560115.SAPP.PDF.

(27) Claridge, T. D. W. High-Resolution NMR Techniques in Organic Chemistry: Third Edition. *High-Resolution NMR Tech. Org. Chem. Third Ed.* **2016**, 1–541. https://doi.org/10.1016/C2015-0-04654-8.

(28) Rosman' And, K. J. R.; Taylor, P. D. P. INTERNATIONAL UNION OF PURE AND APPLIED CHEMISTRY INORGANIC CHEMISTRY DIVISION COMMISSION ON ATOMIC WEIGHTS AND ISOTOPIC ABUNDANCES* SUBCOMMITTEE FOR ISOTOPIC ABUNDANCE MEASUREMENTS** ISOTOPIC COMPOSITIONS OF THE ELEMENTS 1997 (Technical Report) Prepared . *Pure Appl. Chern* **1998**, *70* (1), 217–235.

(29) Gasteiger, E.; Hoogland, C.; Gattiker, A.; Duvaud, S.; Wilkins, M. R.; Appel, R. D.; Bairoch, A. Protein Identification and Analysis Tools on the ExPASy Server. *Proteomics Protoc. Handb.* **2005**, 571–607. https://doi.org/10.1385/1-59259-890-0:571.

(30) Stumpe, S.; Schmid, R.; Stephens, D. L.; Georgiou, G.; Bakker, E. P. Identification of OmpT as the Protease That Hydrolyzes the Antimicrobial Peptide Protamine before It Enters Growing Cells of Escherichia Coli. *J. Bacteriol.* **1998**, *180* (15), 4002–4006. https://doi.org/10.1128/JB.180.15.4002-4006.1998/ASSET/35780B39-6E02-48B5-8194-26620A903E49/ASSETS/GRAPHIC/JB1581244004.JPEG.

(31) Lee, I.; Suzuki, C. K. Functional Mechanics of the ATP-Dependent Lon Protease- Lessons from Endogenous Protein and Synthetic Peptide Substrates. *Biochim. Biophys. Acta* **2008**, *1784* (5), 727. https://doi.org/10.1016/J.BBAPAP.2008.02.010.

(32) Saveliev, S. V.; Woodroofe, C. C.; Sabat, G.; Adams, C. M.; Klaubert, D.; Wood, K.; Urh, M. Mass Spectrometry Compatible Surfactant for Optimized In-Gel Protein Digestion. *Anal. Chem.* **2013**, *85* (2), 907–914. https://doi.org/10.1021/AC302423T.

(33) Lebendiker, M.; Danieli, T. Production of Prone-to-Aggregate Proteins. *FEBS Lett.* **2014**, *588* (2), 236–246. https://doi.org/10.1016/J.FEBSLET.2013.10.044.

(34) Raynal, B.; Lenormand, P.; Baron, B.; Hoos, S.; England, P. Quality Assessment and Optimization of Purified Protein Samples: Why and How? *Microb. Cell Fact.* **2010**, *13* (1), 1–10. https://doi.org/10.1186/S12934-014-0180-6/FIGURES/1.

(35) Kramer, R. M.; Shende, V. R.; Motl, N.; Pace, C. N.; Scholtz, J. M. Toward a Molecular Understanding of Protein Solubility: Increased Negative Surface Charge Correlates with Increased Solubility. *Biophys. J.* **2012**, *102* (8), 1907. https://doi.org/10.1016/J.BPJ.2012.01.060.